Integrated P- and S-Wave Borehole Experiments at the KTB-Deep Drilling Site

E. L. Lüschen
W. Söllner
A. Hohrath
W. Rabbel

INTEGRATED P- AND S-WAVE BOREHOLE EXPERIMENTS AT THE KTB-DEEP DRILLING SITE

E. Lüschen*, W. Söllner*, A. Hohrath*, W. Rabbel**

ABSTRACT

Data are presented from integrated special experiments which have been performed in conjunction with a seismic 3D reflection survey within the framework of ISO89 (Integrated Seismics Oberpfalz 1989) coordinated by DEKORP (German Continental Seismic Reflection Program) between July and November of 1989.

The main objective was to study the nature of P- and S-wave reflections and velocities, the Poisson's ratio and the seismic anisotropy in a medium of crystalline rocks around the KTB site (Continental Deep Drilling Program), where the borehole has reached a depth of 4000 m. A digital 5-unit geophone chain with 25 m spacing and three components was used for downhole recording.

The program described here consists of:
1) shearwave 2D reflection profiling (SCMP) with two 10-12 km long lines crossing the KTB-site, source: 2 horizontal vibrators with different orientations, 3-component recording;
2) shearwave moving source profiling (S-MSP); downhole recording of the source points of the SCMP;
3) vertical seismic profiling (VSP) down to 3660 m with different source azimuths and offsets (zero-offset, 4 km, 8 km); P- and S-wave sources: explosives, horizontal and vertical vibrators, and horizontal hammer techniques.
4) multiple azimuth shearwave experiment (MASE) with 4 km and 8 km offset and horizontal vibrator sources (radial and transversal orientation).

The VSP surveys display steeply dipping reflections, increasing in number below 3000 m depth. Horizontal structures, preferentially seen in the surface profiling, are the exception. Polarization analysis of shearwaves shows dominant azimuths in shearwave splitting which correlate with maximum horizontal stress (N 158° E) and with azimuth and dip of foliation.

---

* Geophysikalisches Institut, Universität Karlsruhe, Hertzstrasse 16, D-7500 Karlsruhe 21, F.R.G.
** Institut für Geophysik, Universität Kiel, Olshausenstrasse 40-60, D-2300 Kiel 1, F.R.G.

INTRODUCTION

The interpretation of standard 2D-reflection profiling data collected in crystalline areas often suffers from the lack of direct calibration. Deeper crustal reflections (e.g. DEKORP Research Group, 1988; Lüschen et al., 1987) differ significantly from those known from industrial sedimentary basin surveys. Although they are often very bright, reflections from crystalline rocks appear discontinuous and of chaotic or, in the lower crust, of laminated character.

The German Continental Deep Drilling Program (KTB) offers a unique opportunity to study seismic reflections of the crystalline basement and their nature in more detail. An integrated seismic survey has been designed under the auspices of DEKORP to provide an extensive data base which is comparable to the techniques used in hydrocarbon exploration, including 3D-reflection surveys and vertical seismic profiling (VSP). This program has been extended by the inclusion of many non-standard experiments, particularly using wide-angle, downhole and shearwave techniques.

Shearwave observations, by means of their polarization and by determination of the seismic anisotropy (Helbig and Mesdag, 1982, Crampin, 1987a,b), in combination with standard P-wave measurements, possess the potential to obtain additional information on lithology and structure, crack and microcrack distribution. Experimental studies by Nur and Simmons (1969) have shown that velocity anisotropy can be induced by the stress field. Laboratory measurements on crystalline samples (Kern, 1982) demonstrated that the Vp/Vs ratio can be a very useful lithological indicator. The KTB offers a direct link between experiments on core samples, well-loging, and seismic illumination by downhole surveys and surface seismic measurements. Thus, seismic images of the crystalline environment can be calibrated by findings in the borehole and, on the other hand, the regional significance of lithological and structural features in the borehole can be tested.

This article describes a package of four special field experiments, completed within the Integrated Seismic Program between July and November of 1989. They focus on application of shearwave and downhole techniques in order to derive information which complements standard P-wave techniques. We used a series of standard and non-standard field configurations, described in the next chapter, as well as supplementary experiments with different source techniques. The basic principles of these techniques, which came into use in industrial hydrocarbon exploration in the eighties, are provided by several excellent review and introductory articles, e.g. Hardage (1985) and Danbom and Domenico (1986).

Our intention was to illuminate the target area around and below the borehole (maximum depth 4000 m) with seismic waves of different resolution characteristics for different angles and raypaths addressing the problem of distinguishing lateral inhomogeneities from seismic anisotropy. The experiments described in this article should not be regarded as stand-alone experiments. Their full resolving power is expected during integration of all experiments, particularly in conjunction with the contemporarily completed 3D seismic survey.

The processing is not yet completed. Particularly, polarization studies require a systematic approach in the future. Therefore, this paper describes the present stage of the data base after completion of most of the standard processing sequence. First noteworthy results are also outlined. Figure 1 shows the area of main interest indicated by a frame of 15 km side length and 15 km depth around the projected KTB-hole. Figure 2 shows the same target area represented by the SW-NE reflection profile KTB 8502 (DEKORP Research Group, 1988), where the KTB-hole is located in its centre. Reflections of almost discontinuous character can be recognized below 0.7 s TWT. The most prominent group of reflections is found between 3 and 4 s TWT, which define the so-called Erbendorf body (Franke, 1989).

THE EXPERIMENTS

Figure 3 represents a location map of all the experiments to be described in this chapter. It covers nearly the same area which has been surveyed by the 3D reflection technique. Figure 4 shows the basic principles applied to each corresponding experiment. All field operations were performed under the technical management of field crew Schwanitz of Prakla-Seismos AG, Hannover, in close cooperation with the authors from DEKORP and with the KTB logging group. SCMP and S-MSP experiments were conducted in July 1989 in the starting phase of the ISO89-program before the 3D-survey. All the others were performed during holidays and weekends of the 3D field crew until late November 1989.

I) Shearwave 2D reflection profiling (SCMP)

The SCMP-experiment has been designed analogous to standard P-wave 2D reflection profiling using the commom-midpoint (CMP) stacking method. We were interested in the near-vertical shearwave response of crustal structures (down to the crust-mantle boundary) known from previous P-wave profiling during the reconnaissance phase (DEKORP Research Group, 1988). The Erbendorf-body, characterized by pronounced P-wave reflectivity and relatively high velocities between 3 and 4 s P-wave two-way traveltime (or approximately 9 to 12 km depth), was of particular interest.

Since it could not be expected to exceed the lateral und vertical resolution of P-waves, this experiment was designed to produce multifold CMP-coverage for two short perpendicular profiles, each approx. 5 km long. CMP-stacking in this case is expected to enhance the shearwave signal to noise ratio and to allow for velocity analyses. The field configuration of the two lines was closely adapted to the previous P-wave profiling of 1985. Its design benefitted from a pilot study in the Black Forest (Lüschen et al., 1990) concerning the efficiency of shearwave generation by the Vibroseis method and by explosions. A comparative study is under preparation.

The layout of the three-component receivers was asymmetric to the source points (see figure 3) in order to enable velocity analysis for greater moveouts and to better balance between the energy of first arrivals and late reflections, which is of crucial importance when using the Vibroseis technique. The deployment of three-component receiver stations,

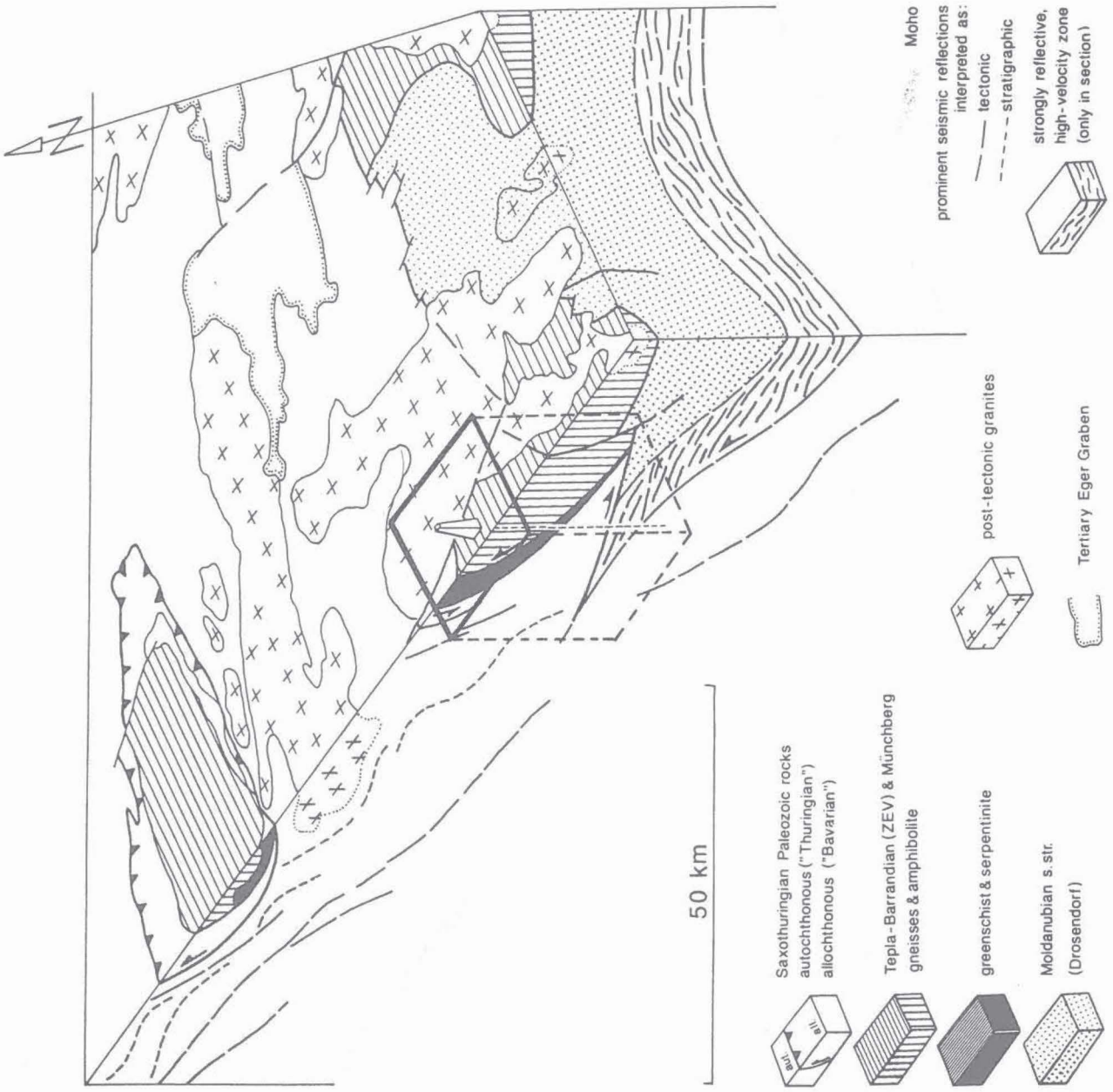

Figure 1: Study area marked by a frame of approximately 15 km side length and 15 km depth. Interpretive 3-D representation of 4 the crustal structure around the KTB drill site derived from surface mapping and 2-D reflection profiling during pre-site investigations (from Franke, 1989). The surface of the marked target area correspondes also to location map of figure 3.

Figure 2: Central part of the stack section KTB 8502 from a pre-site survey (DEKORP Research Group, 1988). Length of section: 12 km, shown are the first 5 s TWT corresponding approximately to 15 km depth. Processed by DEKORP Processing Center Clausthal. Location of KTB is indicated.

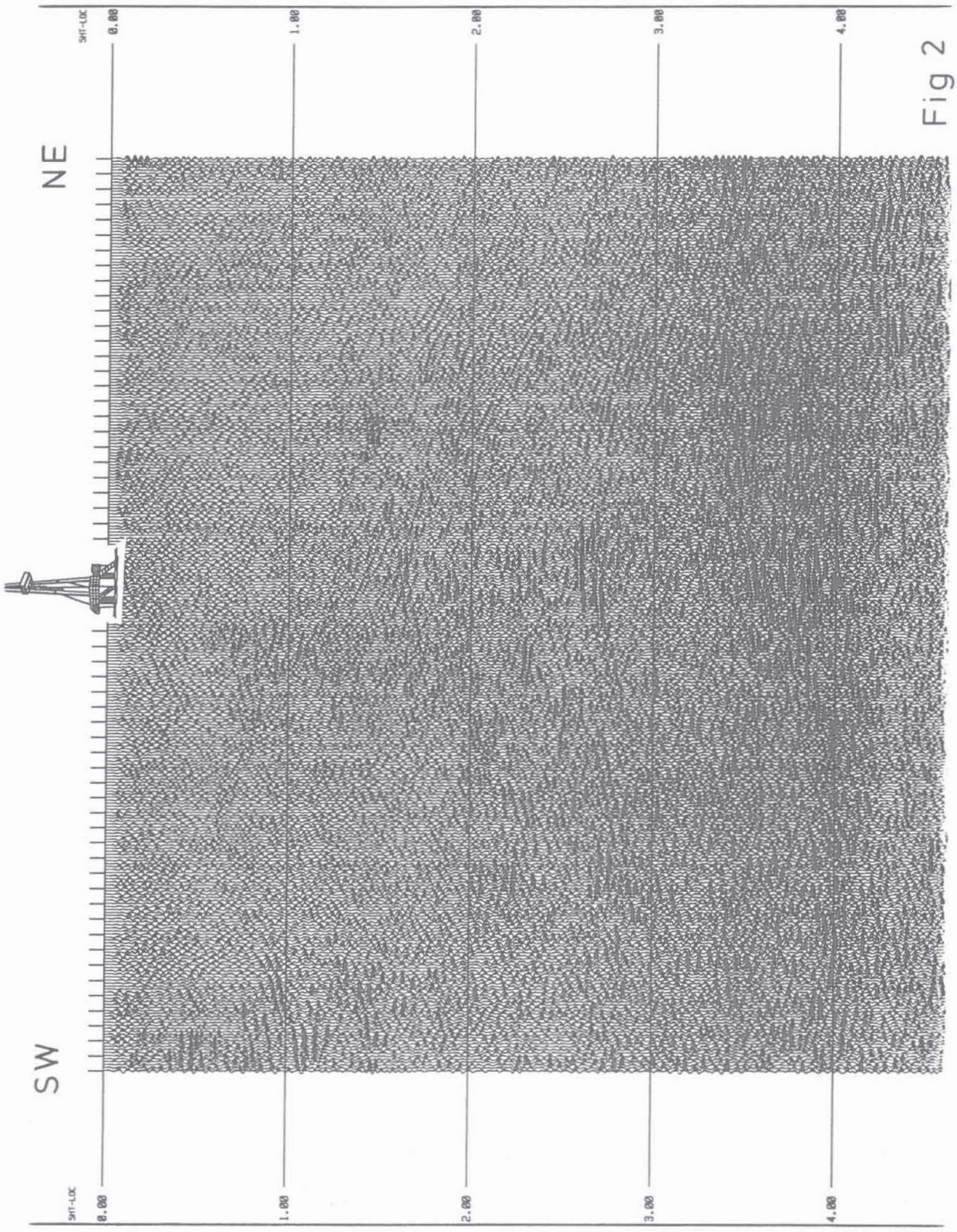

Fig 2

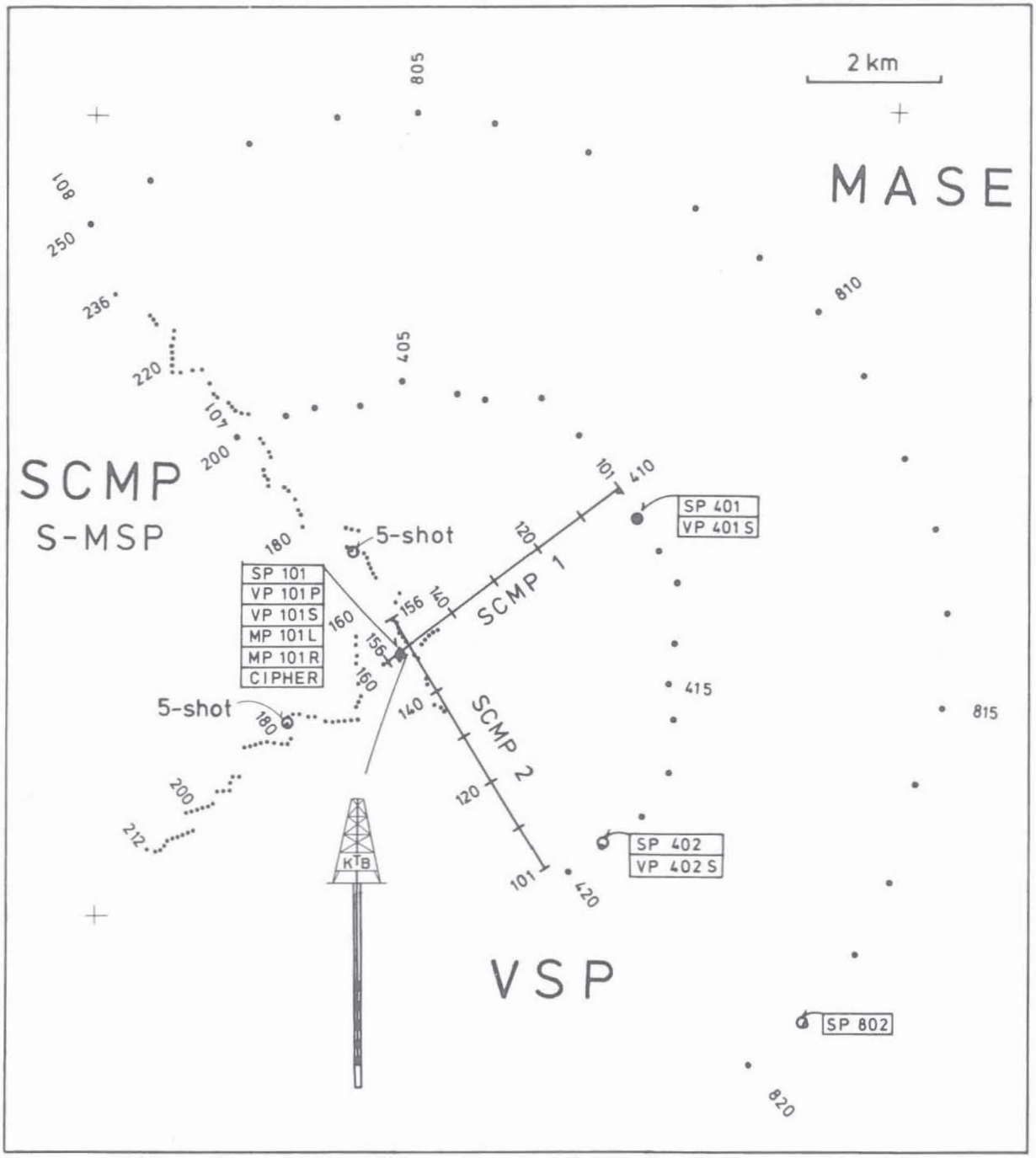
2 km
MASE
SCMP
S-MSP
VSP
5-shot
5-shot
SCMP 1
SCMP 2
SP 101
VP 101 P
VP 101 S
MP 101 L
MP 101 R
CIPHER
SP 401
VP 401 S
SP 402
VP 402 S
SP 802
KTB
805
801
250
236
220
107
200
212
405
810
410
420
415
815
820
101
120
140
156
160
180

Fig 3

Figure 3: Location map of the study area, reduced from scale 1:25000.
SCMP: Shearwave 2D reflection profiling, line SCMP1: locations 101-212 (NE-SW), line SCMP2: locations 101-250 (SE-NW), dots are vibrator points, solid lines are stationary 3-component receiver spreads;
S-MSP: Shearwave moving source profile, simultaneous recording of all SCMP source points with a 3-component downhole geophone unit at 3400 m depth;
VSP: Vertical seismic profiling, 4 source points: 101 (zero offset), 401 and 402 (4 km offset) and 802 (8 km offset), SP: explosive source, VP (P): verticalvibrator, VP (S): horizontal vibrator, MP (L) Marthor source (hammer, left), MP (R) Marthor, right, CIPHER: circular polarized horizontal excitation.
MASE: Multiple azimuth shearwave experiment, vibrator source points 401-420 (4 km offset) and 801-820 (8 km offset).

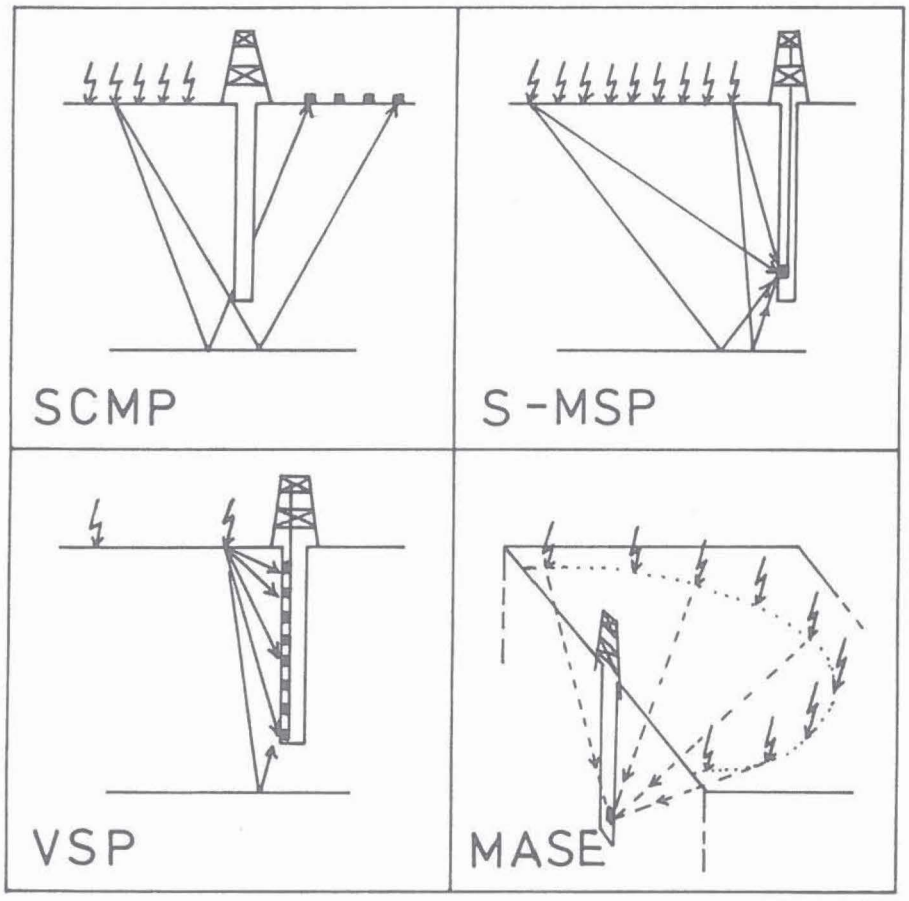

Figure 4: Schematic diagram with the basic principles of the SCMP, S-MSP, VSP and MASE experiments.

particularly of the horizontal geophone strings, needs special care concerning ground coupling and orientation. Therefore we decided to deploy them only once, and rechecked the layout frequently, keeping it in a stationary position, while the source moved along the line. The maximum coverage is therefore produced on a sector with the KTB-hole in its centre and decreases towards the ends of the lines.

The recording was done by two DFS V systems of the DEKORP group at NLfB, Hannover, and the University of Karlsruhe, with a total number of 168 channels, equipped also with stacker and Vibroseis electronics. The spread on each line (SCMP 1 and SCMP 2) consisted therefore of 56 3-component stations (locations 101-156) with a spacing of 80 m.

Two horizontal vibrators (type VVCS, Prakla-Seismos AG) were used as shearwave source. They moved in 80 m intervals from location 144 to 212 (SCMP 1) and from 136 to 250 (SCMP 2). After a start-up sweep test an upsweep of 9 to 43 Hz and 30 s length was choosen, since it turned out to be impossible to generate signal frequencies significantly above 40 Hz. Most vibrator-points were situated in meadows with a relatively hard ground, so ground coupling of the wedge-shaped baseplates was highly efficient, without any ground-damage, and enabled good force and phase control. The orientation of the horizontally vibrating baseplates was transverse (Y) to the line on all points. Additionally, on every third point we also used Y-45° and Y+45° orientations.

In contrast to explosive techniques, vibrators offer the possibility to apply well-defined stresses to the ground regarding their frequency and their orientation. On the other hand, the energy of shearwave generation is not always, except for some favourable cases, comparable to explosive sources and sometimes not predictable. This may be caused by non-optimum ground coupling and by effects ocurring within the weathering zone. This apparent drawback was expected to be compensated during multiple vertical and horizontal (CMP) stacking.

Additionally to the Vibroseis survey, explosives were used on one shotpoint on each line, to produce a single-fold shotgather with the site of the KTB-hole in the centre of the coverage (compare figure 3, shots are labeled with '5-shot'). These shotpoints consisted actually of 5 distinct holes (20-25 m deep, spacing 5 m, one hole in the centre, each one charged with 25 kg dynamite), which were fired, the centre shot first, and recorded separately. According to the three-hole technique (or Camouflet method, Edelmann, 1985), the central shot produces a zone of weakness or a lateral inhomogeneity. The other shots, adjacent to this zone, therefore produce stronger horizontal stresses which then propagate as shearwaves. These shearwaves may be further enhanced when the records of the two opposite shots are stacked after inverting the polarity of one of them. In our case we modified this three-hole method by an additional pair of shots.

For static corrections, a short-refraction survey with a 12 channel signal-enhancement system and an oblique hammer device (VAKIMPAK) for shearwave generation was used on selected parts of the two lines. Additionally, the other experiments, especially the S-MSP, are expected to provide static corrections for shearwaves.

Table 1 lists all important field parameters (Vibroseis survey). The operation was performed in a 2 week campaign at the end of July 1989 during the starting phase of the 3D survey.

Source	2 vibrators VVCS (Prakla-Seismos)		
	170 kN Peak Force, force control		
	wedge-shaped baseplates		
	spacing		80 m
	signal (upsweep)		9 - 43 Hz
			30 s length
	orientation		transversal (Y)
	(on each third point:		Y,Y-45o,Y+45o)
Receiver	three components		
	horizontal components:	Sensor SM 6,	8 Hz
	vertical component:	Sensor SM 4,	10 Hz
	group spacing		80 m
	geophones per group		12
	no specific geophone pattern (5-10 m)		
Recording	TI-DFS V 120 Channel (DEKORP, Hannover)		
	TI-DFS V 48 Channel (University Karlsruhe)		
	both with I/O-MSP Stacker and Pelton		
	Vibroseis electronics		
	2 uncorrelated records per vibrator point and orientation		
	5-fold vertical stack of each record		
	sample interval		4 ms
	length of recording		34 s ,37 s
	pre-amplifier		42 dB
	low-cut		5 Hz or out
	high-cut		62 Hz
	format		SEG B
CMP coverage (after processing)			50-70
	decreasing towards the endpoints of the line		

Table 1: Field parameters used in shearwave 2D reflection profiling (SCMP)

II) Shearwave moving source profiling (S-MSP)

A moving-source-profile (or walkaway survey, compare figure 4) was gathered at the same time as the SCMP survey. This was achieved by recording all SCMP sources simultaneously by a downhole tool. A digital 5-unit geophone chain (SEKAN 5, Prakla-Seismos AG), which very recently has been developed for KTB purposes (Mylius et al., this volume), was placed in a stationary position between 3590 m and 3690 m depth, the spacing being 25 m. Each unit

consisted of 3 components oriented in cartesian coordinates, each component consisted of 2 detectors connected in series. Sensor 10 Hz geophones were used. The signals were filtered on-site, pre-amplified (by switchable gains), A/D converted and transmitted in multiplexed form to the surface. Each unit was equipped with a magnetic compass for orientation.

Recording was done at the KTB-site with a 24-channel ES 2420 EG&G system, borrowed from the Alfred-Wegener-Institut, Bremerhaven. 15 channels were needed for downhole recording. This microprocessor-controlled system allowed for quick preprocessing (e.g. correlation, stacking, filtering etc.) and quality control. The quality of the SCMP source points thus could be evaluated immediately. Recording in slave operation was triggered by the master-DFS V system of the SCMP. Recording parameters were essentially the same. Field data format is SEG D.

For purposes of inspection and repairs the digital chain had to be replaced by an analogue single 3-component unit after the first week. Line SCMP 2 was therefore recorded with this unit.

III) Vertical seismic profiling (VSP)

Vertical seismic profiling provides the closest link in interpretation between reflections observed in 2D and 3D surface reflection profiling and the lithology in the borehole. Its application in hydrocarbon exploration has been widely established during the eighties (Hardage, 1985).

P-wave sources as well as S-wave sources were applied. In order to cover a maximum range of frequencies and corresponding resolution characteristics, different source types for each wave type were also used (see table 2).

The Marthor (trademark of IFP) was used additionally to the vibrator source in order to compare zero-phase signals (after correlation) with minimum-phase (impulsive source) regarding polarization analysis. Since the source was located on very hard ground, higher signal frequencies were expected with the Marthor, but frequencies lower than 40 Hz were actually generated, lower than using the vibrator. Also energy of the Marthor source turned out to be lower than in case of the vibrator. Therefore it was decided to continue with the vibrator technique in the subsequent MASE experiment where a good shearwave signal to noise ratio was of crucial importance.

Four different source locations were used (compare figure 2). Although a high-quality zero-offset VSP already existed (with a dense receiver spacing of 12.5 m, completed in winter 1988/89, actual offset 200 m, see following chapter), another dynamite zero-offset profile (labeled SP 101) was repeated with an offset of 60 m. The reasons for this were, firstly that the processing quality of the old profile (Schruth et al., 1990) has been hampered by the combination of two different datasets, and secondly that borehole-guided waves (e.g. Stonley-waves) could be expected additionally from a source point closer to the borehole. We preferentially considered these wave types relevant for fracture and stress analysis. The S-vibrator VP 101 S was located at the same place, while the other zero-offset sources VP 101 P, MP 101, and CIPHER were located at 160 m, 200 m and 320 m offset. The other three source points 401, 402 and 802 were located at 4 km and 8

km offset, respectively, and in different azimuths (see figure 3). They were considered to provide a link to the MASE-Experiment and to illuminate the target area with a wider range of different raypaths, which is important for inversion techniques and for anisotropy studies.

P-wave sources:

a) dynamite (SP): single charges of 0.5 - 1 kg in 20 m deep holes, which were used multiple times, tamped with water, actual firing depth was variable: 5-20 m, base of weathering zone near 5 m depth, a monitor geophone at 60 m depth was used for signal control.

b) vertical (standard) vibrator (VP (P)): Type VVEA,
Prakla-Seismos, 19 t,
Upsweep 10 - 80 Hz, length 20 s,
vertical stack 5-10-fold, recorded without correlation.

S-wave sources:

c) horizontal vibrator (VP (S)): Type VVCS (see table 1)
Upsweep 9 - 47 Hz, length 30 s, stacked 10-fold (5-fold per record), recorded without correlation, orientation: transverse with respect to source-hole azimuth.

d) Hammer, MARTHOR (MP): Type M 3, Institut Francais du Petrole, 10 shots on each side (left (L), right (R)) were stacked and recorded separately to allow for inverted stack during processing, orientation mostly transversal with respect to source-hole azimuth (SW).

e) CIPHER : Circular polarized shearwave excitation, new method in test, based on Vibroseis technique Edelmann and Lüschen (1990).

Table 2: Listing of seismic source techniques used in the vertical seismic profiling (VSP)

The downhole tool was the same as described above (SEKAN 5). The chain of 5 units (spacing 25 m) first was moved to a defined depth position, then all source points and all sources were recorded subsequently, before the chain was moved by 125 m to the next position. Maximum depth was 3660 m, since in 3766 m a whipstock was set during drilling which could not be passed. Recording of the whole sequence took about 45 to 60 min and moving the downhole chain was accomplished in another 10 min (including reading of the magnetic compass). Recording was done again with the 24-channel ES 2420 EG&G system already mentioned above. Parameters, such as sampling rate, length of record, stacking, correlation etc., often had to be changed from record to record. Sampling rates of 1 ms were used for dynamite sources and the Marthor, 2 ms for the P-wave vibrator and 4 ms for the S-wave vibrator.

A first set of profiles was acquired during August 1st-4th working 18 hours each day: profiles SP 101, VP 101 S, MP 101, SP 401 and VP 401 S. Signal to noise ratio was found to be relatively low in this time period. Inspection

of the downhole chain indeed revealed damages to cables and electronics due to corrosive borehole fluids.

Within a second time period, from October 30th to November 3rd, the profiles VP 101 P, SP 402, VP 402 S and SP 802 were recorded with the cable material of the downhole unit replaced by more resistant materials. Data quality has improved considerably, particularly regarding the signal to noise ratio of the data behind the first arrivals.

The CIPHER experiment (see table 2, Edelmann and Lüschen, 1990), testing a special vibrator configuration to generate circular polarized shearwaves, was conducted shortly after the MASE experiment (see next chapter) on 6th September. A vertical profile from 2800 m to 3400 m depth was recorded with the SEKAN 5 downhole tool during this experiment. This shearwave source was also applied on selected vibrator points of the SCMP and S-MSP experiments.

IV) Multiple azimuth shearwave experiment (MASE)

Shearwave sources were distributed over half-circles around the KTB-hole, with special emphasis on the analysis of azimuth-dependent anisotropy. Two circles of 4 km and 8 km radius, respectively, were selected, starting NW over E to SE, each one with 20 source points (see figure 3). The far-offset source points of the VSP were also located on these half-circles.

After a comparative study between the Vibroseis and the Marthor source during the first VSP-experiment, mentioned above, we favoured the vibrator for shearwave generation because of its higher energy. One vibrator (VVCS) was used for radius 4 km and 2 vibrators for radius 8 km. Additionally, at a radius of 2 km, 5 vibrator points (separated by 45°) were recorded with one vibrator (not shown in figure 3). At each point the transverse (Y, with respect to source-borehole azimuth) orientation of the baseplate movement was recorded first und then the radial (X) orientation. An upsweep of 9 to 47 Hz was used with a length of 20 s. Two uncorrelated records were generated per point and per orientation, each one with 5-fold vertical stacking and 32.7 s length.

The downhole tool of 5 geophone units (SEKAN 5) was located at 3300-3400 m depth, with 25 m spacing, during the whole experiment. Thus 15 channels were recorded, three components for each of five units. Recording was done again with the 24 Channel ES 2420 EG&G system. For reference purposes, in order to control the quality of the downhole equipment by checking the reproducibility, a sweep of a stationary vibrator nearby the borehole was recorded from time to time. This experiment was conducted from the 2nd-6th of September. While one vibrator was operating at a radius of 4 km, the others at a radius of 8 km were moving to their next position and were operating alternately with the first vibrator.

At each source point an extensive shallow shearwave refraction survey was conducted by a group from Kiel University. The object was to correct static effects on time delays and anomalies in polarization caused by the near-surface weathering layer. Horizontal geophones were deployed at intervals of 2 m along 200 m long lines. A manual hammer was hit horizontally on an

iron bar clamped to the ground. Recording was done by a 24-channel microprocessor-based system (own construction).

Additionally, a near-surface polarization experiment (NESPE) was conducted at several source points of the MASE. Its objective was to study anomalies in polarization caused by near-surface effects. Single down-sweeps of 41 to 11 Hz and 61 s length were recorded. The vibrator was rotated in several steps of 45°. The analysis will be based on first arrivals.

DATA PROCESSING AND FIRST RESULTS

The present stage of processing is described and first results and phenomena are outlined. The sequence of experiments is the same as in the previous chapter. The processing is being performed with a CONVEX C1 super-computer and DISCO software at Karlsruhe University.

I) SCMP

The field layout was planned to enable CMP-processing as a tool to enhance signal to noise ratio of deep S-wave energy. Because the spread was not rolled (stationary), the highest CMP coverage is achieved near the center of the two lines, close to the borehole. Crooked line processing has to be applied. Major problems are expected from the topography and from highly variable near-surface velocities and weathering thickness. We therefore consider static corrections as a very crucial processing step. If this is not appropriately done, the quality of CMP stacking will decrease drastically inspite field records with a relatively high signal to noise ratio.

Since static corrections are not yet available, we present single vibrator-point gathers regarded as typical from both lines. Figures 5 and 6 show 3-component gathers of vibrator-point 170 of line SCMP1 and VP 197 of line SCMP2, respectively (compare figure 3). Processing only consisted of demultiplexing, correlation, vertical stacking of 2 field records, combining records of DFS V 48 channel and 120 channel systems. No further processing has been applied, the data show true amplitudes.

P-wave onsets of the direct wave can be seen on the vertical component, while the horizontal components reveal stronger S-wave first arrivals. Although the source orientation was transversal (Y), the energy of the recorded S-waves is shared by all three components. This indicates strong heterogeneities in the subsurface which cause seismic energy scattering and complex changes in polarization of S-waves. The direct waves of lines SCMP1 (SW-NE) and SCMP2 (NW-SE) are characterized by different phase velocities (table 3). Although the offset range is slightly different in the two VP-gathers, there is first indication of a pronounced seismic anisotropy.

Line	Azimuth	Vp	Vs	Vp/Vs
SCMP 1	N 225	5050 m/s	2950 m/s	1.71
SCMP 2	N 135	5950 m/s	3300 m/s	1.80

Table 3: Phase velocities derived from direct P- and S-waves

Travelling in NW direction, both wave types show increased velocities and an increased Vp/Vs ratio of 1.8 (crustal average is 1.73). These values are representative for a depth range of approximately 1 - 2 km around the KTB site. The difference in Vp is 16 %, in Vs 11 %. This is confirmed independently by a velocity evaluation of the S-MSP data (compare next chapter). A possible relationship of this azimuthal anisotropy with the recent stress field and/or the fracture orientation must be considered. An alternative explanation in terms of lateral heterogeneities, e.g. the granite-gneiss contact, is less likely. The raypaths considered here pass the ZEV (Zone Erbendorf Vohenstrauss) body consisting of gneisses and amphibolites (see figure 1).

Both records also reveal distinct seismic energy on the horizontal components, particularly at 7 s TWT, presumably S-wave reflections. There is no energy seen on the vertical component. The subsurface covered by reflections is nearly identical in the center of the spreads, but different in azimuth. The reflected energy therefore corresponds to the same structure. The signal characteristics are different. On line SCMP1 (figure 5) there is a 0.4 s long band of energy, on line SCMP2 (figure 6) distinct phases, one on each component, can be recognized. Obviously, these elements are different in polarization by 90 degrees. We argue that these phases might be split shearwaves, propagating through an an-isotropic medium above the reflecting structure. This must be substantiated by further polarization analysis of the complete dataset.

Figures 7 and 8 show comparative results of the S-wave Vibroseis (10-fold vertical stack) and the dynamite source for both lines. The field configuration is nearly identical, for comparison see figure 3. Both figures present the raw shot gather in their lower panel, a low-pass filtered version (according to the sweep frequencies used for Vibroseis) in the middle panel and the Vibroseis data of figures 5 and 6 in the top panel. Although the dynamite data reveal better signal to noise ratio of the first arrivals, the later S-wave reflections seen on the Vibroseis horizontal components seem to be of higher quality. On the other hand, the vertical component of the dynamite data show very pronounced P-wave reflections between 3 and 4 s TWT. These reflections correspond to the previously defined 'Erbendorf'-body (see figure 2). Assuming an average Vp/Vs-ratio of 1.73, these P-wave reflections correspond also to the S-wave reflections at 7 s TWT mentioned above. A more detailed study of Lüschen et al. (1990) aims at quantitative comparisons between the spectra of

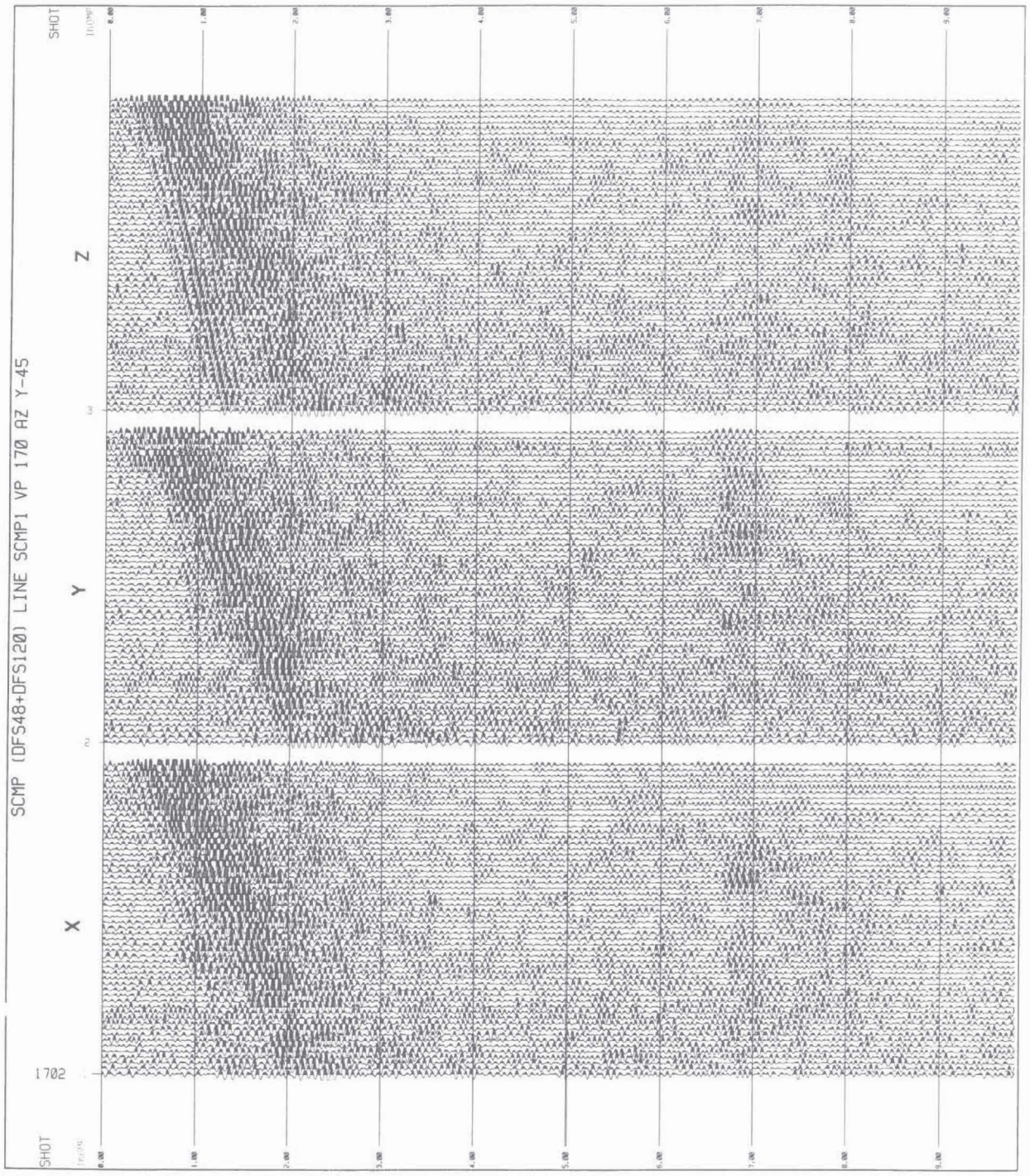

Fig 5

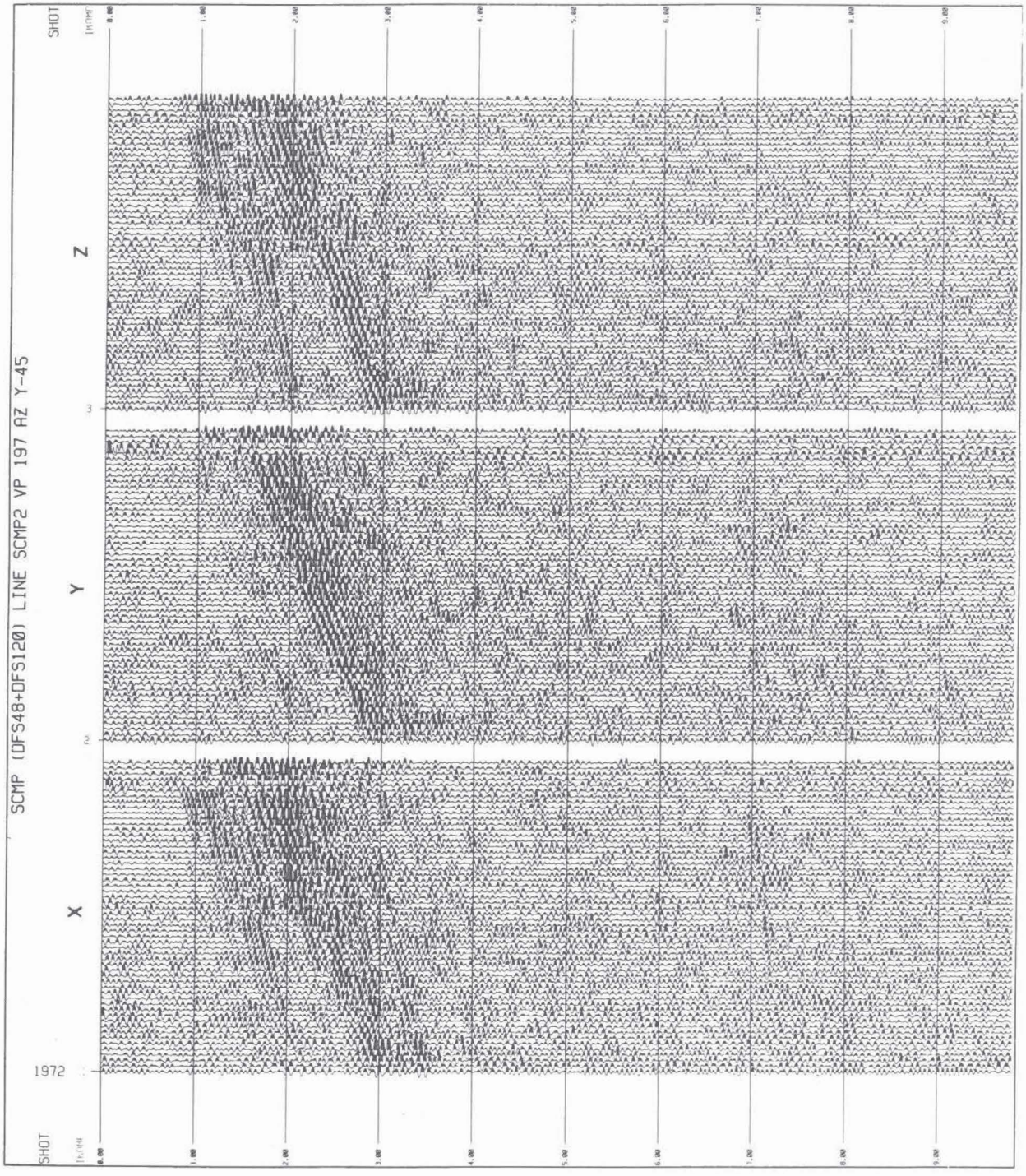

Fig 6

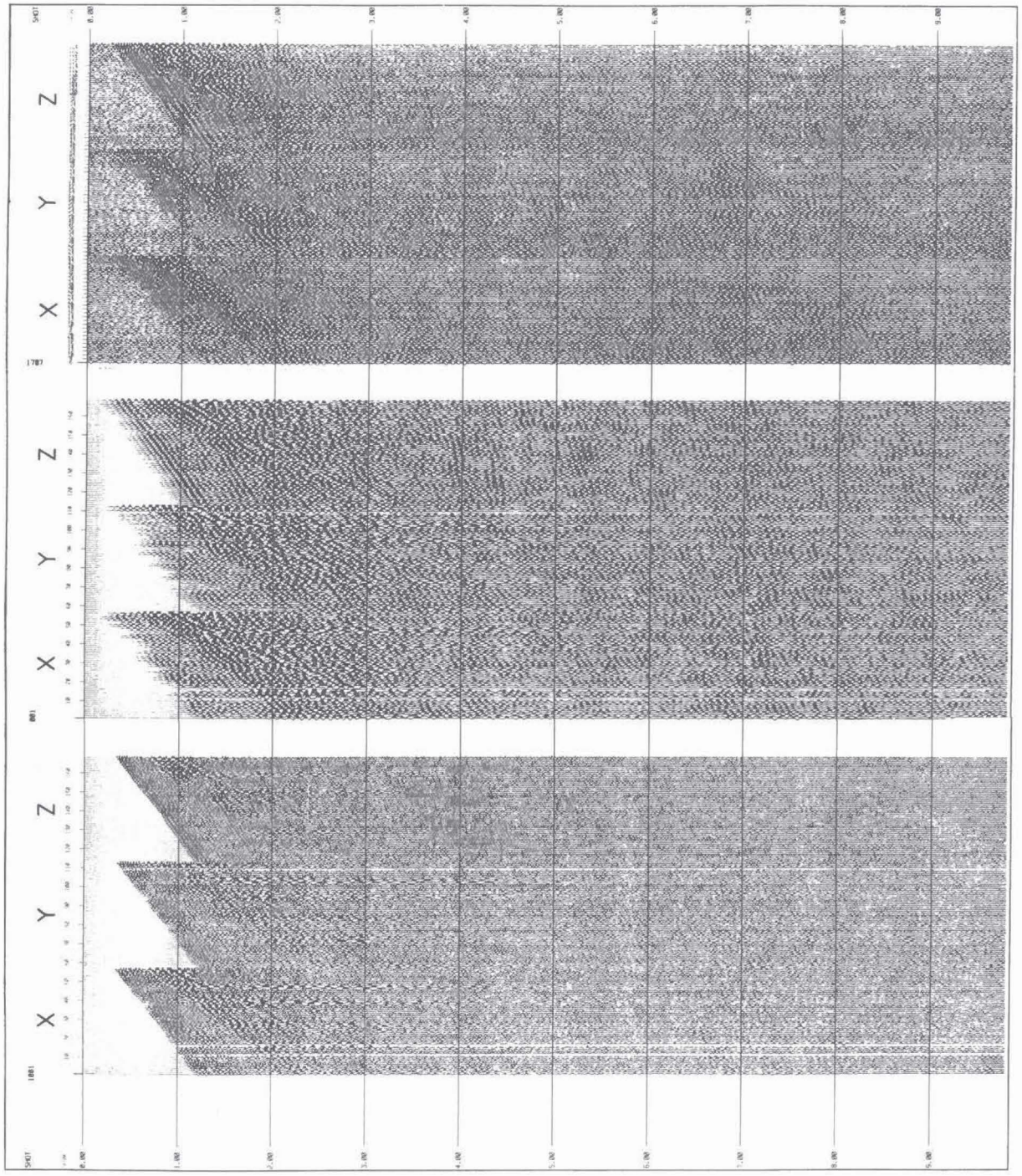

Fig 7

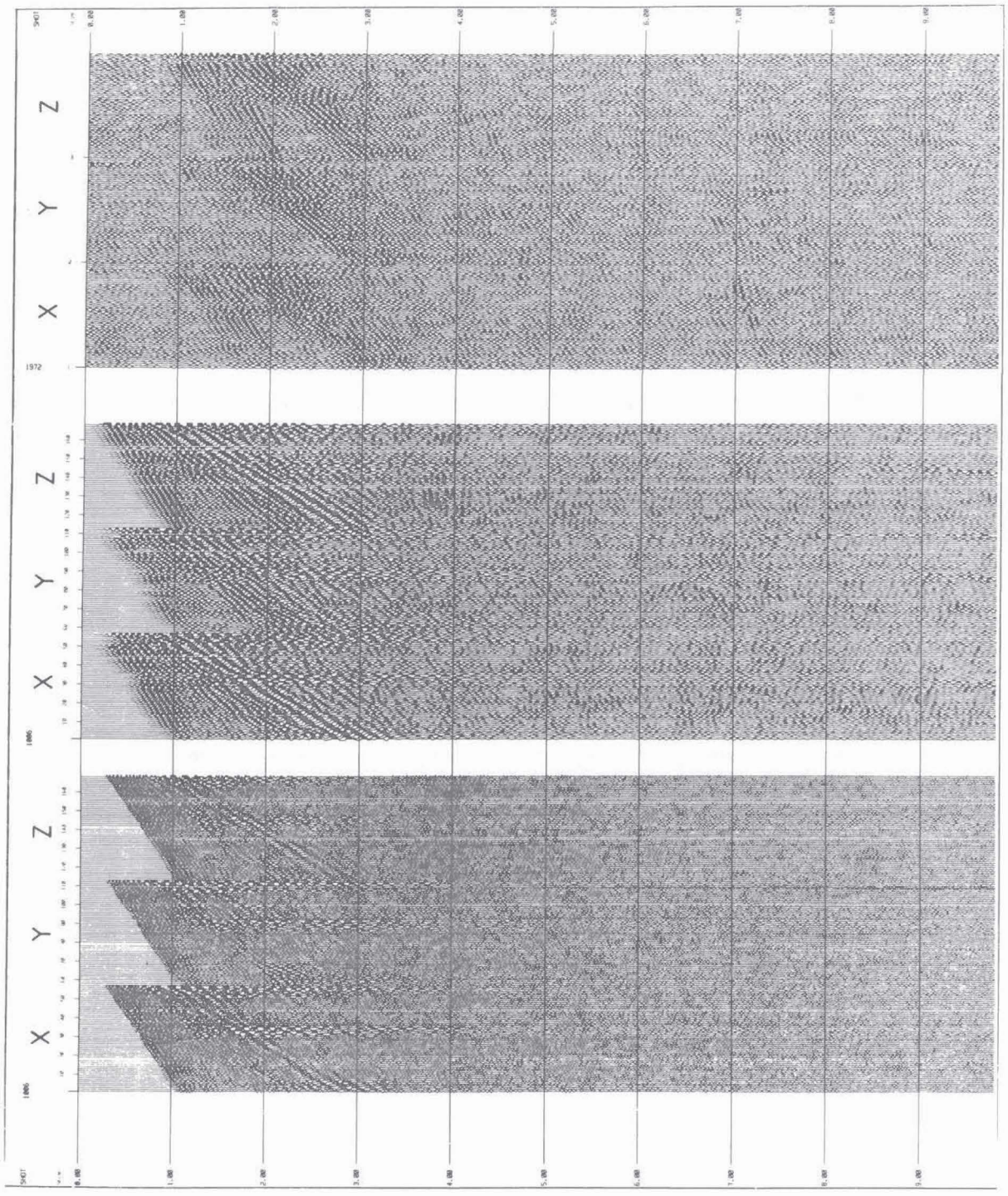

Fig 8

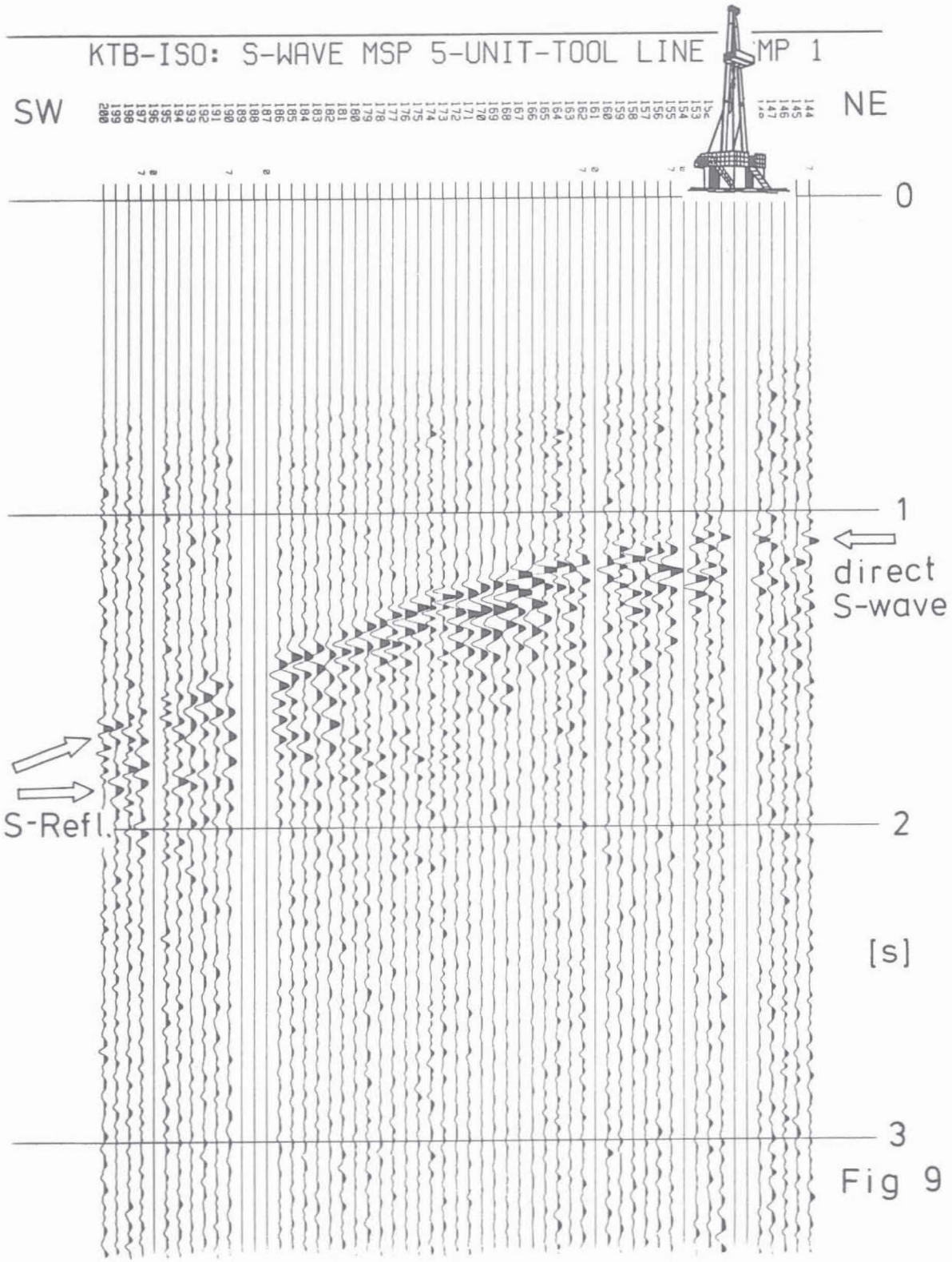
KTB-ISO: S-WAVE MSP 5-UNIT-TOOL LINE
MP 1
SW
NE
0
1
direct
S-wave
S-Refl.
2
[s]
3

Fig 9

Figure 5: Vibrator gather of VP 170 of line SCMP 1. 56 stationar channels for each component. Offset range is from 1.2 km to 5.6 km. Orientation of the vibrator baseplate is transverse (Y). Data were demultiplexed, correlated (extended correlation), 10-fold vertical stack (2 field records). No further processing. True amplitudes. Note highly correlated P-wave first arrivals on the vertical component and less correlated direct S-wave onsets on the horizontal components. S-wave reflections at 7 s TWT.

Figure 6: Vibrator gather of VP 197 of line SCMP 2. Offset range is 3 km to 7.4 km. See figure 5 for more details.

Figure 7: Dynamite-Vibroseis comparison for line SCMP 1. left: raw dynamite data, 25 kg, 1 hole 25 m deep, offset range 1.8 km to 6.2 km.
middle: low-pass filtered version of dynamite data, 9 - 43 Hz.
right: Vibroseis gather of figure 5, 10-fold vertical stack.
Compare P-wave reflections at 3-4 s TWT and S-wave reflections at 7 s TWT.

Figure 8: Dynamite-Vibroseis comparison for line SCMP 2. For details see figure 3 and 7.

Figure 9: Moving source profile (or walkaway) with the shearwave sources of the SCMP survey. The traces are recorded with a horizontal component (H1) located in 3665 m depth (selected from 5 units, located between 3590 and 3690 m, with 3 components each). Note hyperbolic-like direct S-wave arrivals and later arrivales marked in the figure. True relative amplitudes.

different source techniques used in this program. The three-hole technique, taking all shots of one shotpoint into account, provides even better signal to noise ratio for the first arrivals, particularly a better S-wave to P-wave energy ratio, and eliminates the surface waves (Raileigh-wave, seen on X- and Z-components). Quality of deeper reflections could not be enhanced with this technique.

II) S-MSP

The shearwave moving source profile (or walkaway survey) was accomplished during the SCMP survey, recording the vibrator source with a stationary downhole geophone chain. Figure 9 shows an example of the first line representing a horizontal component (H1) of the second unit (of 5 units), located at 3665 m depth with an azimuth of N 2° (H2 at N 92°). The traces correspond to the vibrator location moving from NE (location 144) over the KTB-site to the SW (location 200).

The processing consisted (analogue to data presented in figures 5 to 8) of demultiplexing, vertical stacking of two records, correlating, trace selection one per record. Amplitudes in this presentation are conserved, no further processing has been applied. Zero traces for missing vibrator locations have been added. Since the downhole tool was an array of five 25 m spaced units, each one with 3 components (oriented arbitrarily), 15 datasets of this kind are available for the line SCMP 1 (line SCMP 2: 1 unit with 3 components only). Because of cross-feed during recording by the pilot sweep channel, which produce autocorrelations of the sweep on each seismic channel after correlation, the first 500-700 ms of the record have been muted.

The direct shearwave arrivals seen between 1 and 2 s traveltime, form a typical hyperbola-like curve. Based on the CMP-concept, this allows for a velocity analysis similar to the move-out analysis in surface reflection studies. Such an analysis gives a shearwave velocity of 3130 m/s for line SCMP1 (figure 9) and 3240 m/s for line SCMP2. These velocities must be regarded as average velocities for the medium around the borehole between surface and downhole receiver. The discrepancy confirms the findings from the SCMP direct waves mentioned above. After normal move-out correction of the arrival times, short-period deviations can be usedadvantageously for calculating static corrections for the SCMP survey. Also, later S-wave arrivals are seen on the traces of the southwestern vibrator locations behind the direct arrivals (marked in figure 9). Arriving nearly at the same time from about 25 vibrator positions (arrivals are aligned horizontally), they may be interpreted as reflections from a steep (40-60o) structure dipping to the east.

III) VSP

The processing first had to account for differing recording parameters, such as recording length, sampling rate and number of recorded channels, in the sequence of field records. During the field experiment, the downhole tool was kept in a fixed position while recording all source locations and source types successively, then moved to the next position. The **basic processing** is as follows. During demultiplexing (format SEG D,

multiplexed), the data were sorted into their appropriate profiles. In case of Vibroseis, the data were vertically stacked (2 records) and then correlated (in two versions: zero-phase correlation, minimum-phase correlation). The correlation length was extended by adding zero samples at the end of the uncorrelated records.

Figure 10 demonstrates the problems related to application of dynamite sources. Shots were repeated in the same hole several times. Therefore coupling conditions as well as the depth of the charge vary along the profile. The upper panel shows the variation of **source signature** as well as delays in arrival times recorded with the monitor geophone located at 60 m depth beneath the source. The same characteristics can be recognized in the middle panel representing raw first arrivals recorded downhole which have been time shifted in or der to be aligned horizontally. Signal signature as well as arrival times change drastically. Application of spiking deconvolution (lower panel) can compensate for these artificial variations of the signal characteristics.

Vibroseis as well as Marthor data were not affected by this problem. On the other hand, the dynamite data contained much higher frequencies enabling higher resolution. At about 1100 m depth, seen in the raw data, a tube wave starts downward. Its origin marks the position of a major breakout in the borehole wall known from caliper logs.

Figure 11 describes the next major processing step which is typical for 3-component VSP processing: the **rotation of components** (e.g. Toksöz and Stewart, eds., 1984). This is demonstrated in figure 12 on the data of VP 402 (S-wave vibrator, 4 km offset). The 5 downhole units were orientated arbitrarily during recording and movement in the borehole. The upper panel of figure 12 represents the raw original data set for far-offset VSP 402 (compare figure 3 for location). Consistent and correlating phases can be recognized on component Z (labeled IKOMP = 1). The shearwave energy is dominant, also weaker P-wave energy can be seen.

The middle panel of figure 12 shows the three components after rotation (see e.g. DiSiena et al., 1984; Benhama et al., 1988) according to the compass readings. Component 1 (right) is still vertically orientated, component 2 (formerly H1) now is northward, and component 3 (left, formerly H2) now is eastward orientated. Shear-wave phases now show good correlation on all three components. Since the azimuth of the raypath is NW, P-wave energy is distributed on all three components of this North-East oriented cartesian coordinate system.

The lower panel shows the components in a different coordinate system, which is orientated according to the raypath direction. Component 1 is now the radial one (parallel to source-receiver direction). P-wave energy is now concentrated on this component, as theory predicts. Component 2 is horizontal radial (HR) and component 3 is horizontal transversal (HT). This rotation can be performed automatically using two methods (after DiSiena et al., 1984; Kanasewich, 1981; Benhama et al., 1988):

1) Maximizing the energy. First, P-wave energy is maximized within the horizontal plane, searching for the rotation angle which maximizes the P-

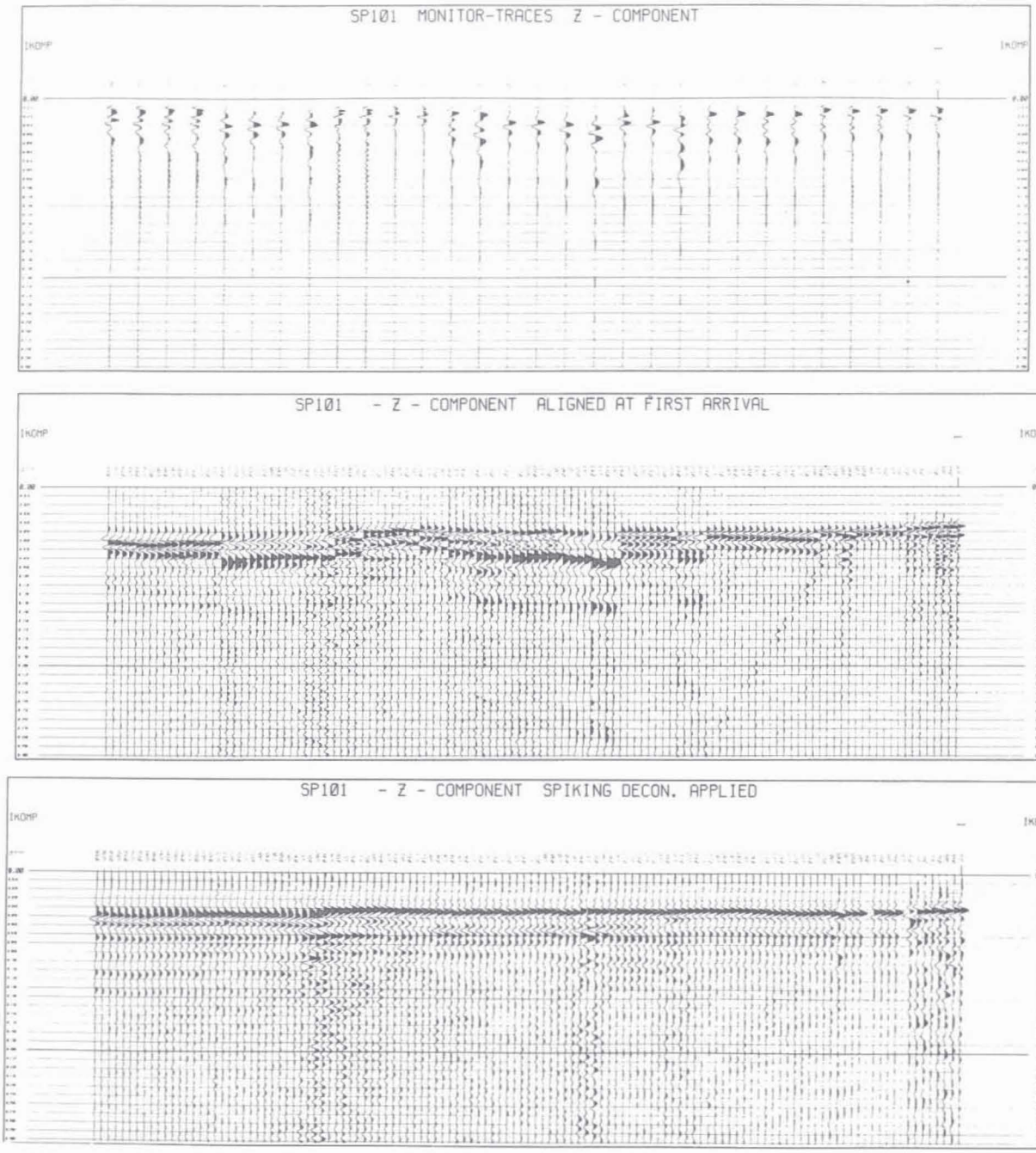
SP101 MONITOR-TRACES Z - COMPONENT
IKOMP
IKOMP
SP101 - Z - COMPONENT ALIGNED AT FIRST ARRIVAL
IKOMP
IKOMP
SP101 - Z - COMPONENT SPIKING DECON. APPLIED
IKOMP
IKOMP

Fig 10

Figure 10: Zero-offset VSP SP 101 (dynamite, z-component): Comparison between monitor traces (upper panel) with downhole geophone traces (middle panel). Note strong variations in signal signature and arriving times. Traces of the downhole record are shifted upward to be aligned horizontally. Note the tube wave starting at 1100 m depth. Lower panel: downhole data after application of spiking deconvolution.

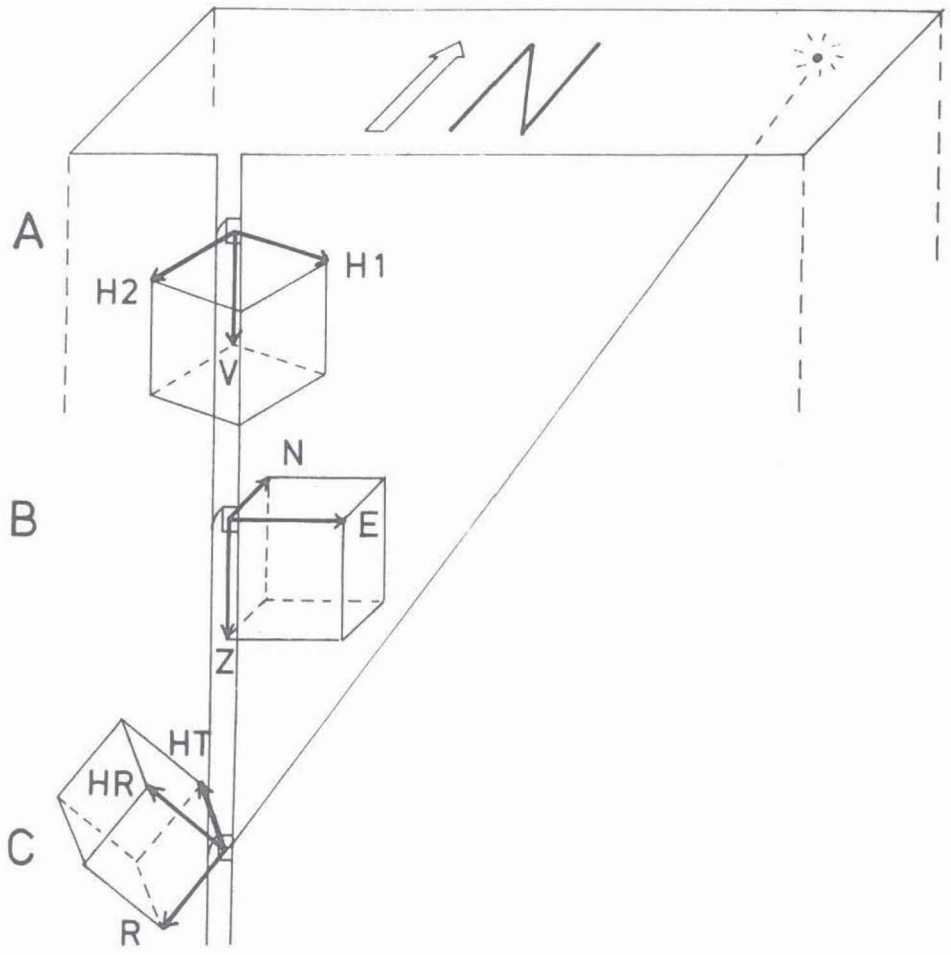

Figure 11: Schematic diagram of different coordinate systems used for rotation of the recorded wavefield. A: original arbitrary coordinate system, B: rotated system according to compass readings, C: rotated system using automatic procedures described in the text.

Figure 12: Far-offset vertical seismic profile VP 402. Source offset 4 km, source: 1 S-wave vibrator, source azimuth SE. Top: three components of raw data, original receiver orientation (not orientated). 1=Z, 2=H1, 3=H2. Middle: rotation according to compass readings, 1=Z, 2=N, 3=E. Bottom: rotation using the covariance matrix, 1=R, 2=HR, 3=HT.

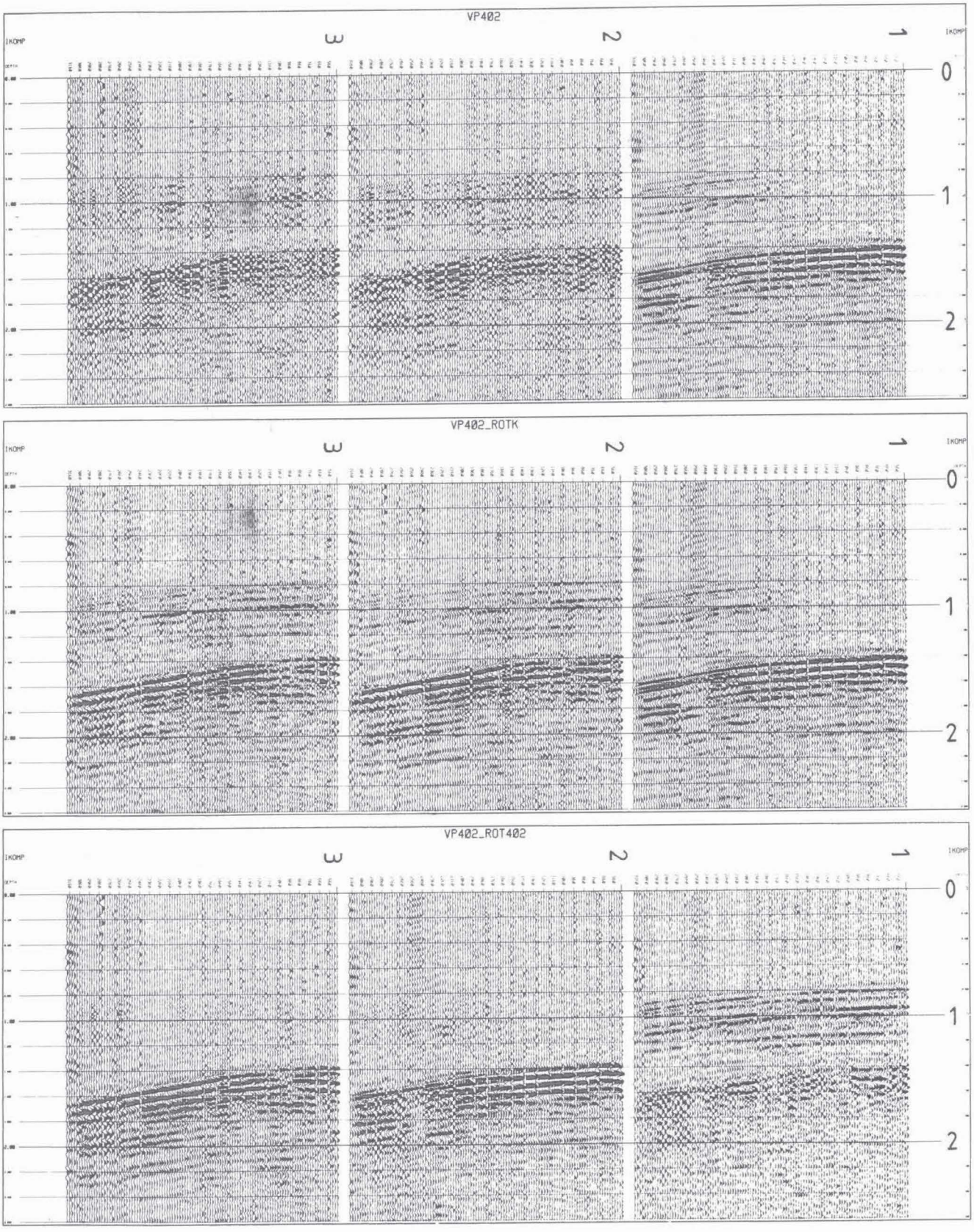
VP402
IKOMP
3
2
1
IKOMP
0
1
2
VP402_ROTK
IKOMP
3
2
1
IKOMP
0
1
2
VP402_ROT402
IKOMP
3
2
1
IKOMP
0
1
2

Fig 12

wave energy on the horizontal radial component (H1 -> HR). Then this procedure is repeated for the HR-Z-plane (Z -> R).
2) Covariance matrix. From the covariance matrix the minimum variance is determined instead of maximizing the energy.

Both methods are basically related to each other, and produce practically the same results. For automatic rotation we use the method with the covariance matrix. This method additionally provides the degree of rectilinearity of the polarization. It is used simultaneously with the rotation after compass readings, depending on the individual problem to be studied. The automatic rotation requires that P-wave energy is present on all components. In contrast to earlier suggestions, figure 12 also shows that the compass provides reliable readings.

The next crucial processing step is **deconvolution**. This is of particular importance for all zero-offset VSPs. The Vibroseis data in this case need to be transformed from zero-phase to minimum-phase signals, which in our case is done during correlation. An operator of 1000 ms length is applied to the downgoing wavefield first. The antifilter is then applied to the complete wavefield. Thus the resolution of the signals is enhanced and multiples are suppressed.

Figure 13a presents the original wave field of all available zero-offset VSPs in a compressed and comparative form. First, all traces have been shifted down by a constant time, then the traces were individually shifted upward according to the traveltime of the direct S-wave. For better comparison, this procedure alignes the shearwaves horizontally. On top of figure 13a the data of the previous VSP 3600 (Bram, 1988, Kästner et al., 1989, Hohrath, 1990, Schruth et al., 1990) is also plotted. This data was recorded with a smaller spacing of 12.5 m instead of 25 m and its source signature provides higher resolution, particularly in the case of S-waves.

Thus, five different zero-offset VSPs are now available. It can be clearly recognized, that the S-wave energy and signal frequencies change drastically between the different source types. Additionally, several P to S conversions are visible starting at the P-wave branch of the direct arrivals, particularly on the VSP 3600 (figure 13b). The direct S-wave, which originates at the surface, is propagating in different phases of their own velocity. This is a first manifestation of shearwave splitting according to seismic anisotropy. The slowest phases also could be interpreted as Stoneley waves (borehole guided wave). But this interpretation is very unlikely, because the amplitude decay is typical for body waves and because there are no such waves reflected from the bottom of the borehole. Although the vibrator and the Marthor source were oriented transversly with respect to the source-borehole azimuth, the recorded S-wave energy is not restricted to the HT-component. This indicates that polarization of the signal is changing along its raypath due to the complexities and the anisotropy of the medium. In case of the dynamite sources, the S-wave generation is most likely due to conversion of the P-wave at the surface or at lateral inhomogeneities near the source (Fertig, 1984). In case of the first VSP with 200 m offset (explosive source, top of figure 13a), the slowest shearwave phase cannot be traced upward back to the origin in time and space. It starts with a delay of approx. 150 ms. We

suggest that it is generated by the arrival of the surface wave (Rayleigh wave) at the borehole mouth. For the vibrator and the Marthor, the shearwaves can be regarded as originating directly at the source.

The data shown in figure 13a reveal different S-wave wavelengths and frequencies covering a wide range (10 to 100 Hz). This allows for analysis of the polarization as a function of the frequency. Figure 14 presents a blow-up of VP 101 P. The two split shearwaves can clearly be recognized. Hodograms of the corresponding signals, presented in figure 15, clearly show, that the faster and the slower shearwave are different in polarization by 90 degrees. This means that the S-wave with particle motion in NW direction is faster than the other. Because of the dramatic difference in character between the two phases, the slower one could be interpreted alternatively as a tube wave. But no reflection from the borehole bottom confirms this interpretation. Further systematic analysis of polarization of all our data for more details is necessary to verify these statements.

Figure 16 shows raw data of the CIPHER experiment, represented as a vertical seismic profile with a limited depth range from 2800 to 3400 m. After rotation according to the compass readings, the data show very pronounced and several distinct shearwaves. The P-wave is discernable on the vertical component. Because of better signal to noise ratio, we consider this technique as a powerful tool for generating shearwaves. A detailed study describing the field procedure and the results are under preparation by Edelmann and Lüschen (1990).

Figure 17 and figure 18 show the far-offset VSPs in comparison between the dynamite and the S-vibrator source (see figure 3 for location). P-waves as well as S-waves show the characteristic bending of the first arrival curve, which is due to the larger offset. S-waves are of remarkable quality, especially on the VP 402 S (figure 18). There are several remarkable details to interprete. In SP 401 (figure 17, top), SP 402 (figure 18, top) and SP 802 (figure 18, bottom) there are oblique events between first P-waves and first S-waves, propagating with an almost constant phase velocity, starting when the first P-wave arrives at the borehole mouth. A possible interpretation of this feature is due to a reflection of the direct P-wave at a steeply dipping structure, which outcrops near the borehole site. The reflected wave then propagates vertically along the borehole. Interpretation as a tube wave is unlikely because of the high phase velocities (> 5000 m/s).

In case of zero-offset VSP **wavefield separation** techniques can be applied to suppress the downgoing wavefield (direct waves) and to enhance the upgoing reflections (e.g. Hardage, 1985). Usually, f-k filter or median filters are applied for this purpose. For interpretation purposes, the traces are then time shifted according to the two-way-traveltime correction. After performing a corridor stack, the VSP now can be compared directly with a surface reflection profile. On the other hand, these seismic measurements now can be calibrated by the borehole measurements. Up to this processing stage the date are presented in this paper. Table 4 provides a listing of typical standard processing steps, in this case for the dynamite-VSP SP 101.

S P - 1 0 1

UPGOING WAVEFIELD (P)
FILTER 40 - 110 HZ

FIELD EXPERIMENT

1 SOURCE: DYNAMITE (0.5 - 1 KG)
IN 5 - 20 M DEEP HOLES
OFFSET 50 M

2 RECEIVER: 5-UNIT-DIGITAL 3-K CHAIN
S E K A N
(PRAKLA-SEISMOS AG)
SPACING 25 M

3 3-K MONITOR GEOPHON IN 60 M DEPTH

4 RECORDING UNIT: EG&G GEOMETRICS 2420 (24CH)

5 FIELD PARTY: SCHWANITZ / PRAKLA-SEISMOS AG
LUESCHEN / KARLSRUHE UNIVERSITY

6 DATE: AUG. 1ST-3RD. 1990

DATA PROCESSING HISTORY

PROCESSED BY: WALTER SOELLNER, EWALD LUESCHEN
ACHIM HOHRATH, MARTIN WIDMAIER

CONVEX-DISCO TEAM UNIVERSITY KARLSRUHE

DATE: FEB. 20TH 1990

SOURCE FILE: /MNT/WALTER/PROC/SP101/SP101NPROC.DAT

DATA FILE: /SCRATCH/WIDE/SP101_NSPIKE_UP.DAT

1 DEMUX (FIELD TAPES UNSORTED IN SEGD MULTIPLEXED)

2 BAD TRACE EDIT

3 DEFINITION OF IKOMP DEPTH AND TYPE

4 SORT (INTO PROFILE-IKOMP GATHER)

5 POLARITY EDITING AND ADDITION OF MISSING TRACES

SOURCE FILE /SCRATCH/WALTER/SP101_NSPIKE_UP.DSK 6000

DATA FILE /MNT/EWALD/VSPMASE/VSP_READ_PLOT.DAT

6 ROTATION OF COMPONENTS ACCORDING TO DIRECTION OF DOWNGOING P-WAVE

7 DECONA SPIKE OP.LENGHT 500 MS , DESIGN-GATE 1000 MS

8 F-K FILTER (UPGOING WAVEFIELD PASSING)

9 NOTCH FILTER 50 HZ 100 HZ

10 FREQUENCY FILTER:

TIME RANGE	LOW CUT		HIGH CUT	
SECONDS	HZ	HZ	HZ	HZ
ALL	25	40	110	140

11 MUTE: 625/112 3660/618

12 GAIN: EXPONENTIAL GAIN CORRECTION

13 AGC 300 MS

14 PLOTTING INFORMATION: 6.25 MM PER TRACE
15 CM PER SECOND
POLARITY: POSITIVE PEAKS SHADED
SETAMP: PEAK
GAIN: 3

U N I V E R S I T A E T
K A R L S R U H E

K T B O B E R P F A L Z V B
V S P D A T A P R O C E S S I N G

UNIVERSITAET KARLSRUHE

KTB

Table 4

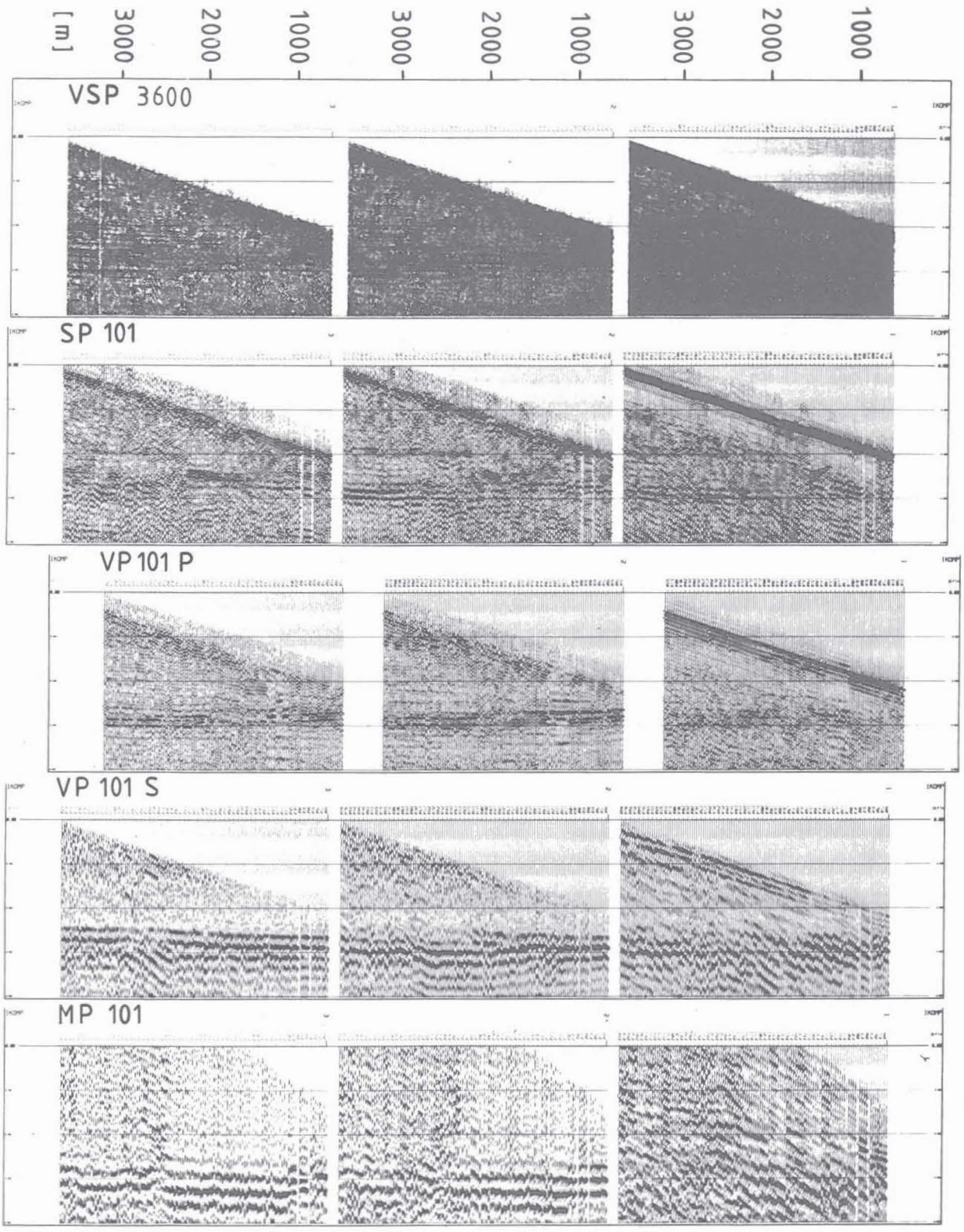
[m]
3000
2000
1000
3000
2000
1000
3000
2000
1000
VSP 3600
SP 101
VP 101 P
VP 101 S
MP 101

Fig 13a

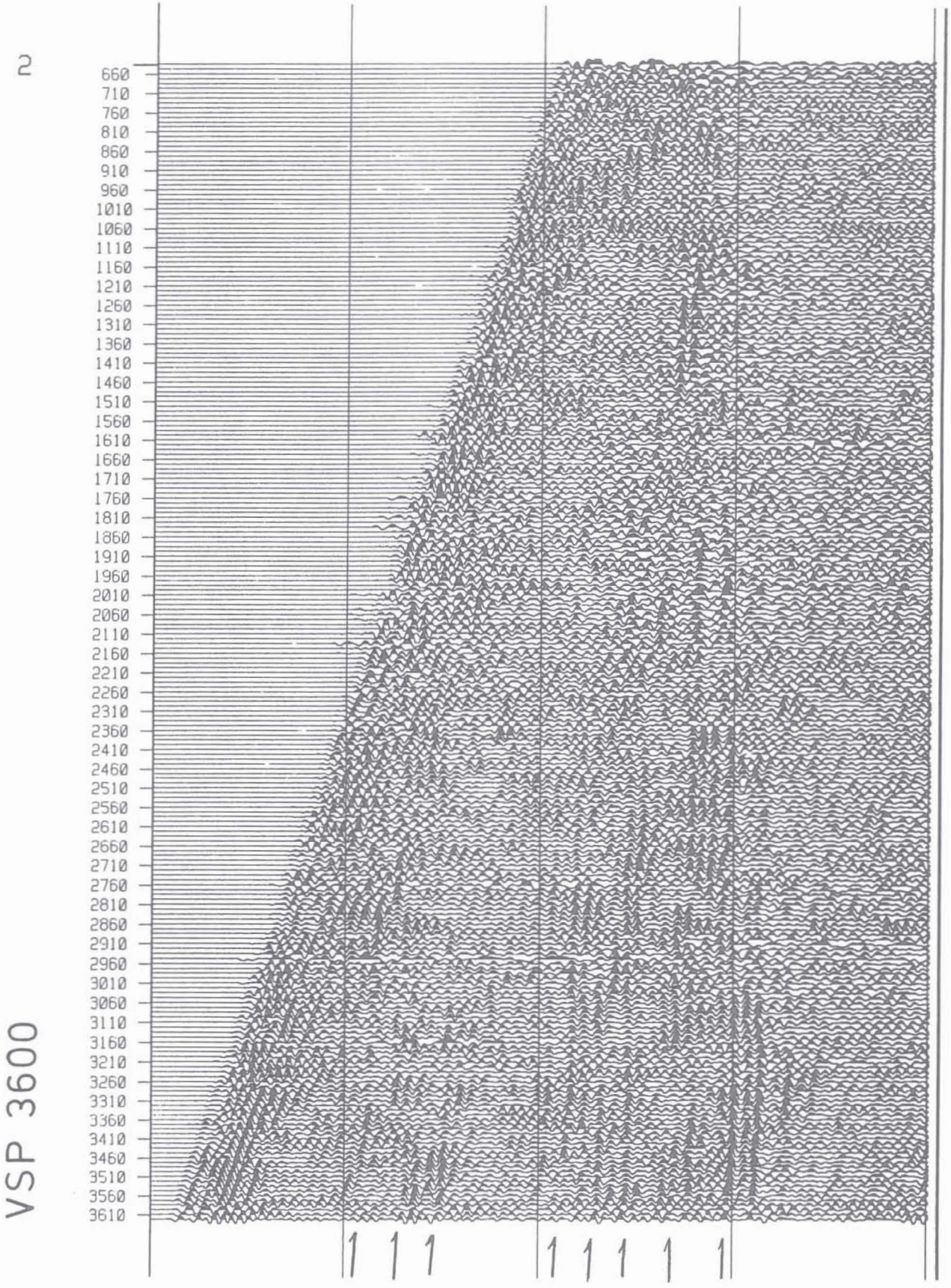
VSP 3600
660
710
760
810
860
910
960
1010
1060
1110
1160
1210
1260
1310
1360
1410
1460
1510
1560
1610
1660
1710
1760
1810
1860
1910
1960
2010
2060
2110
2160
2210
2260
2310
2360
2410
2460
2510
2560
2610
2660
2710
2760
2810
2860
2910
2960
3010
3060
3110
3160
3210
3260
3310
3360
3410
3460
3510
3560
3610

Fig 13b

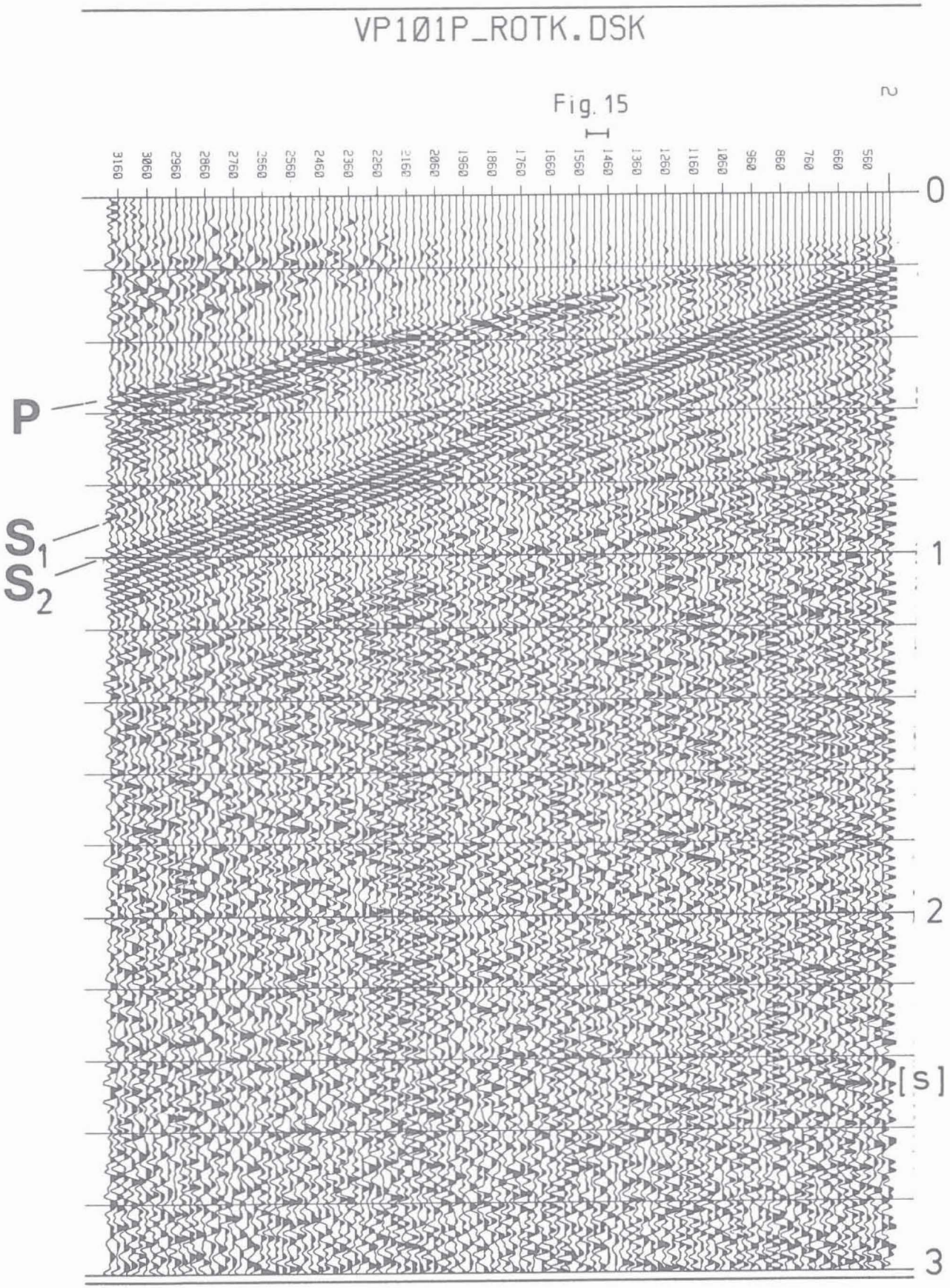

Fig 14

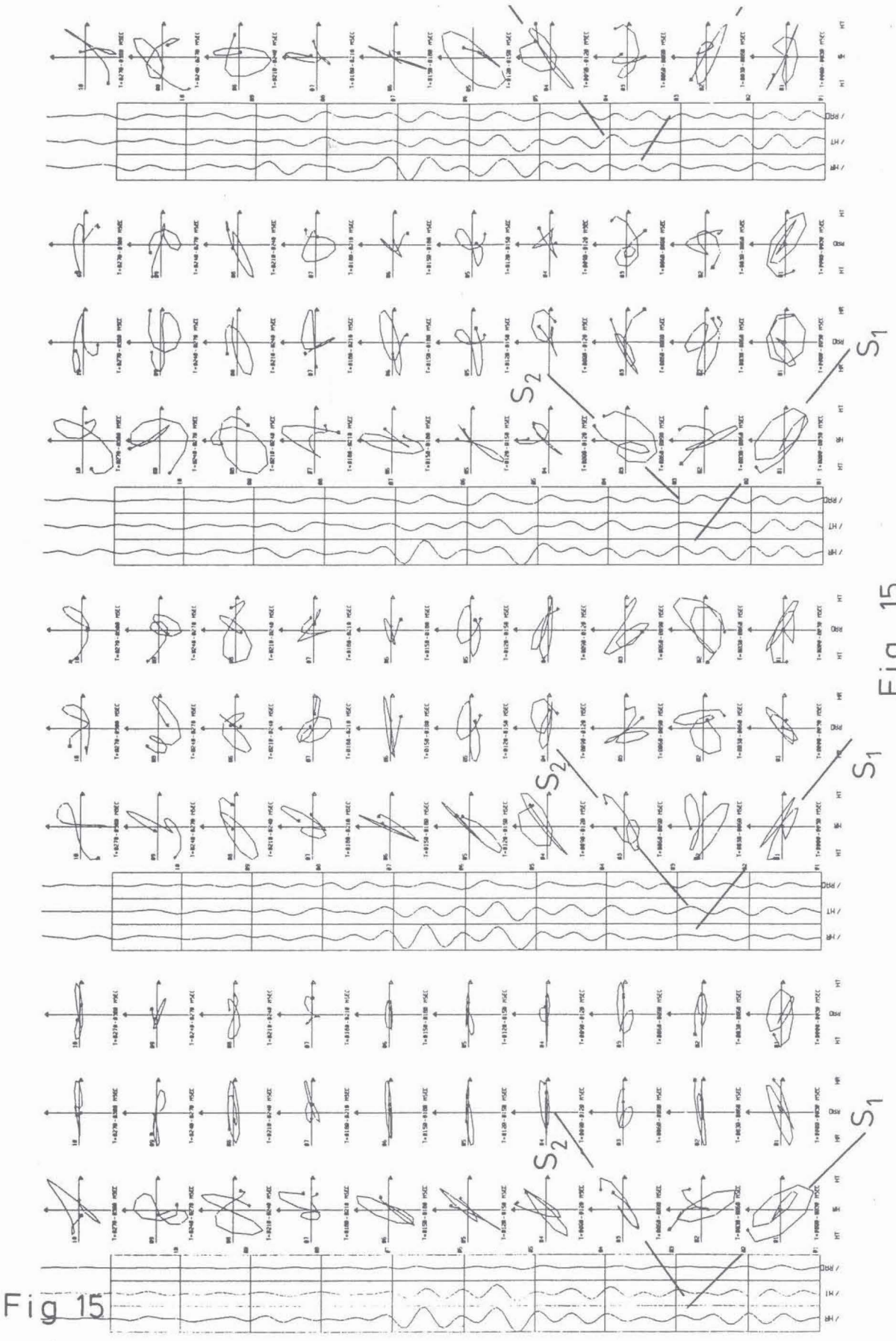

Fig 15

Fig 15

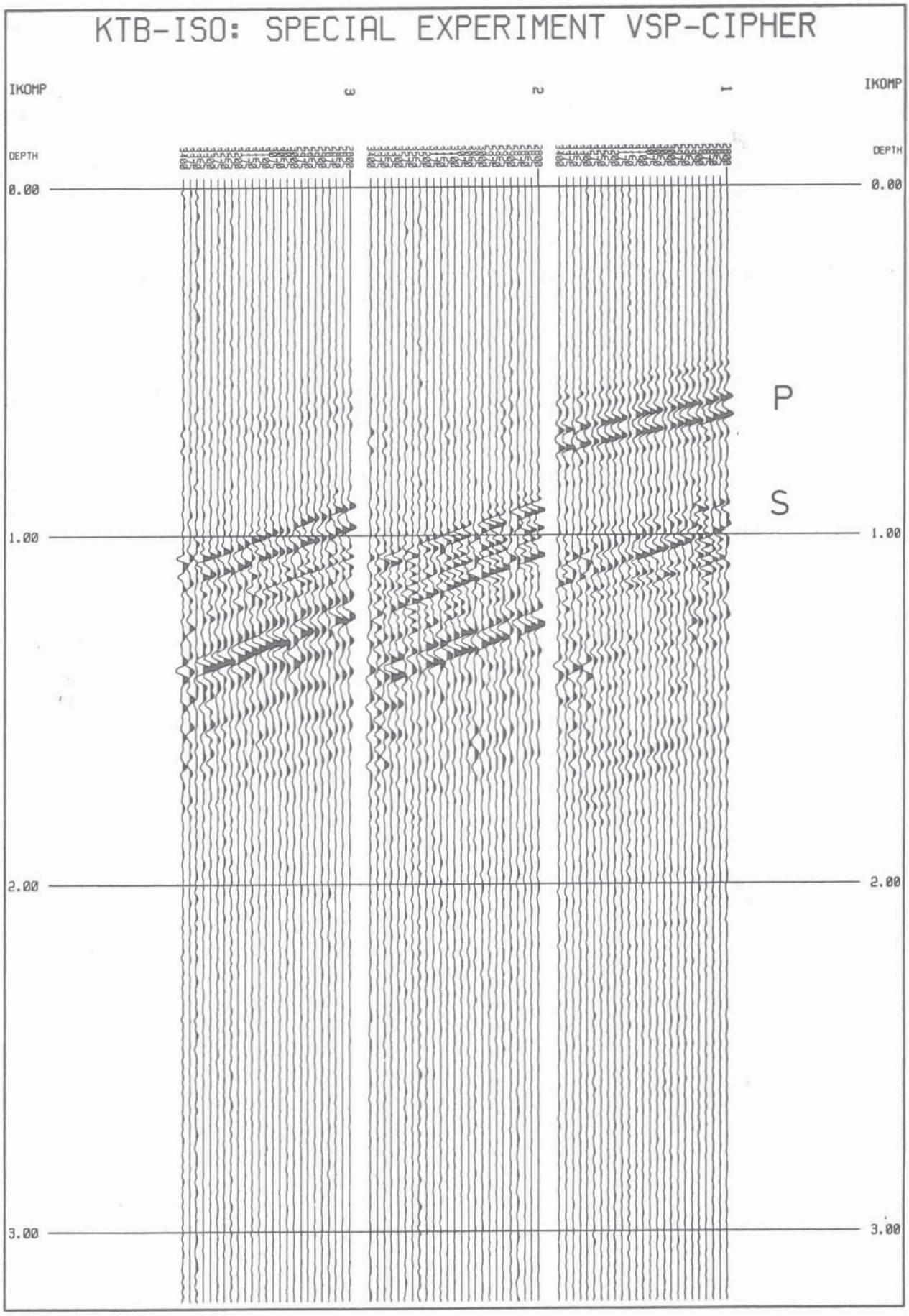
KTB-ISO: SPECIAL EXPERIMENT VSP-CIPHER
IKOMP
3
2
1
IKOMP
DEPTH
DEPTH
0.00
0.00
P
S
1.00
1.00
2.00
2.00
3.00
3.00

Fig 16

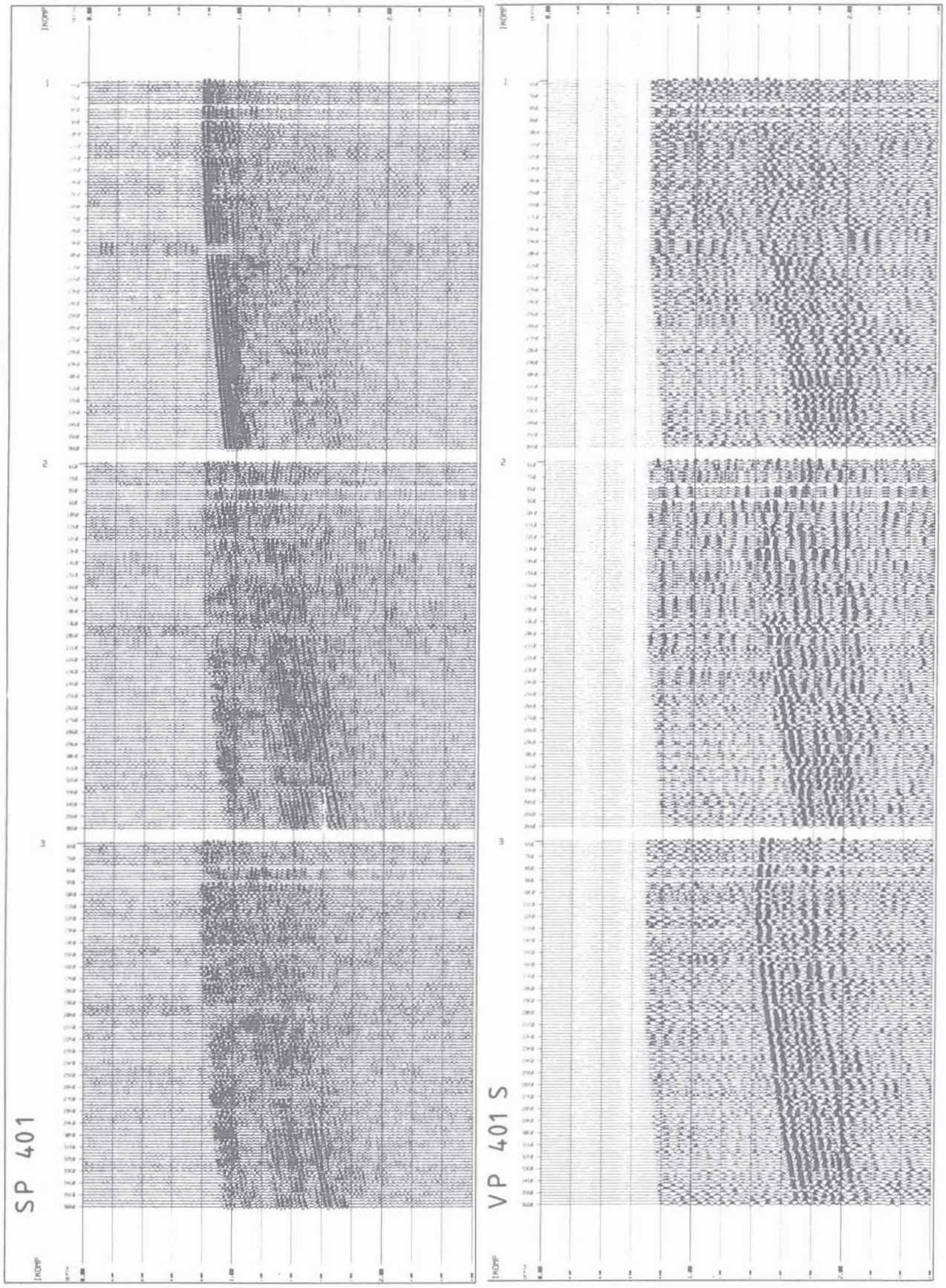

Fig 17

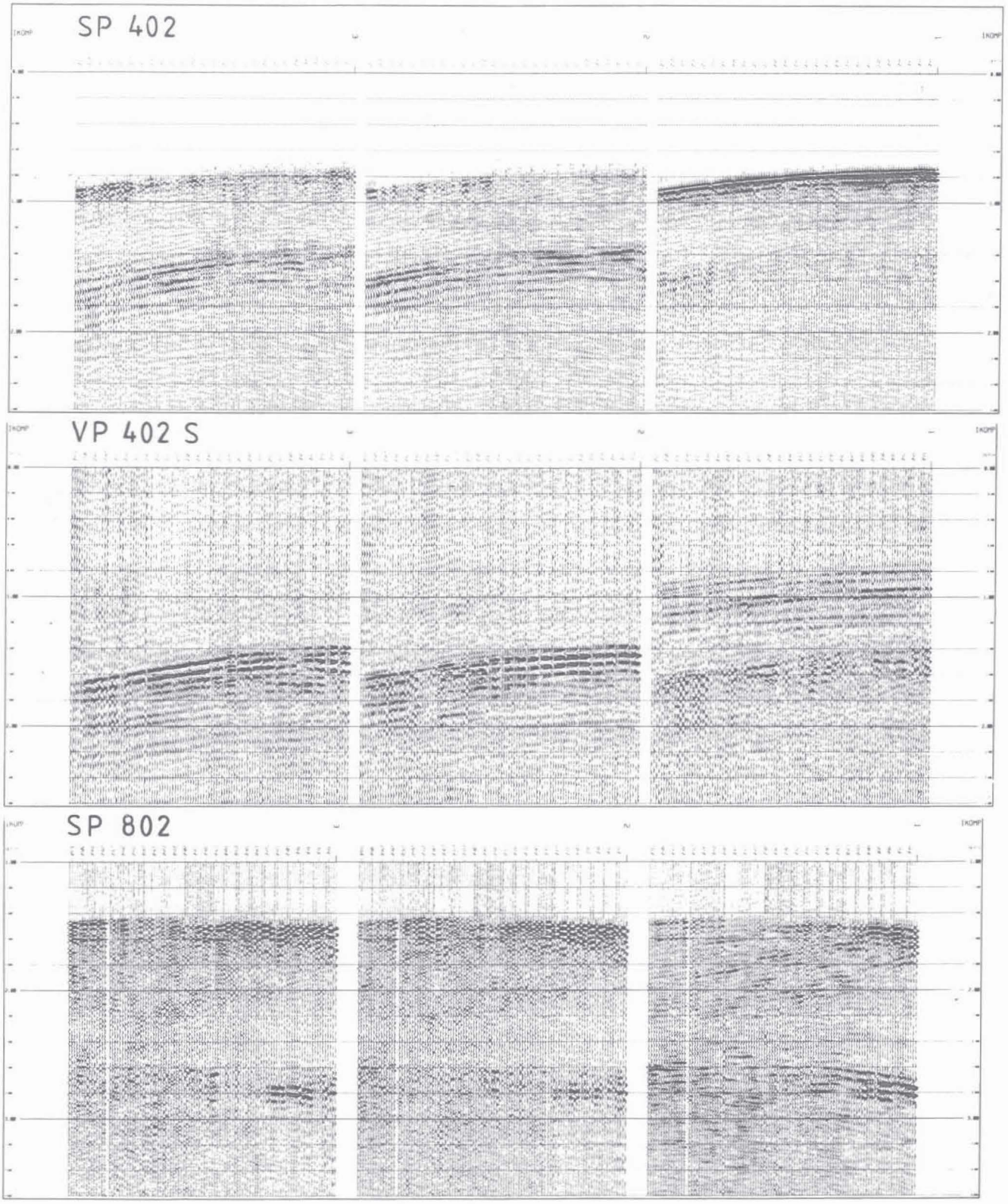

Fig 18

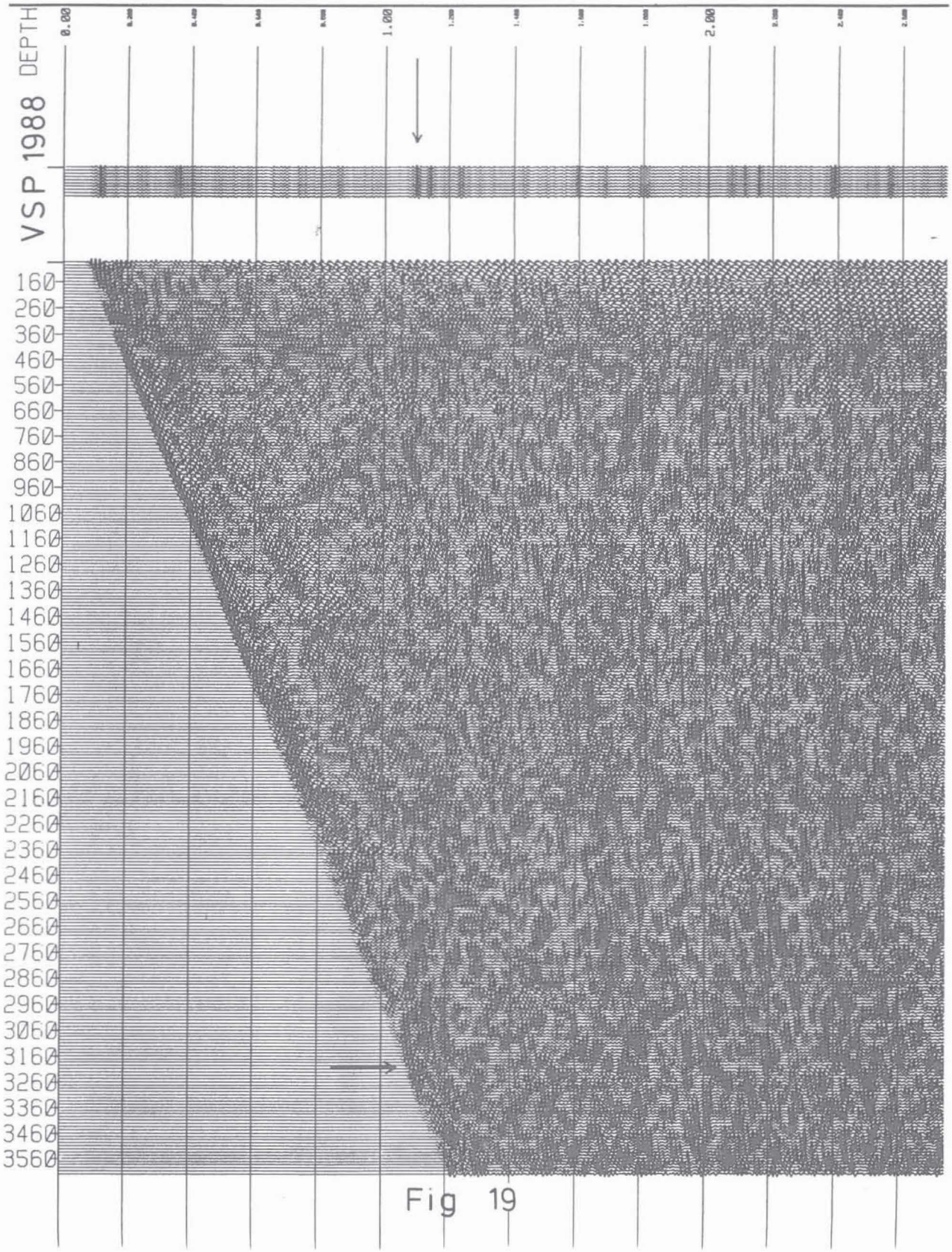
VSP 1988 DEPTH
0.000
1.000
2.000
160
260
360
460
560
660
760
860
960
1060
1160
1260
1360
1460
1560
1660
1760
1860
1960
2060
2160
2260
2360
2460
2560
2660
2760
2860
2960
3060
3160
3260
3360
3460
3560

Fig 19

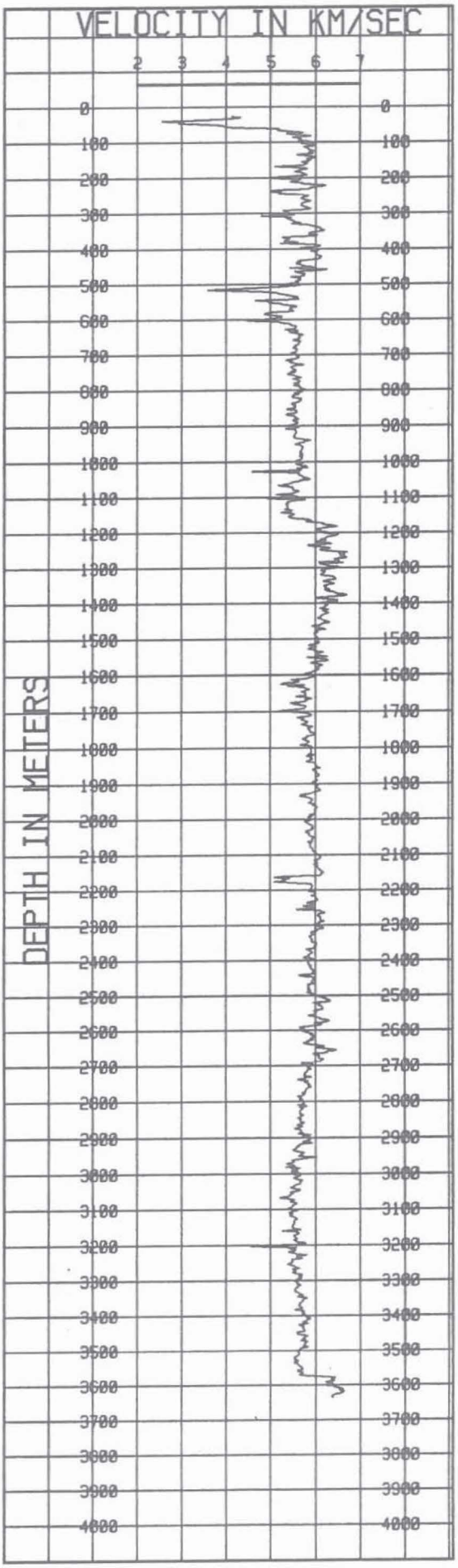
VELOCITY IN KM/SEC
2
3
4
5
6
7
DEPTH IN METERS
0
100
200
300
400
500
600
700
800
900
1000
1100
1200
1300
1400
1500
1600
1700
1800
1900
2000
2100
2200
2300
2400
2500
2600
2700
2800
2900
3000
3100
3200
3300
3400
3500
3600
3700
3800
3900
4000

Fig 20

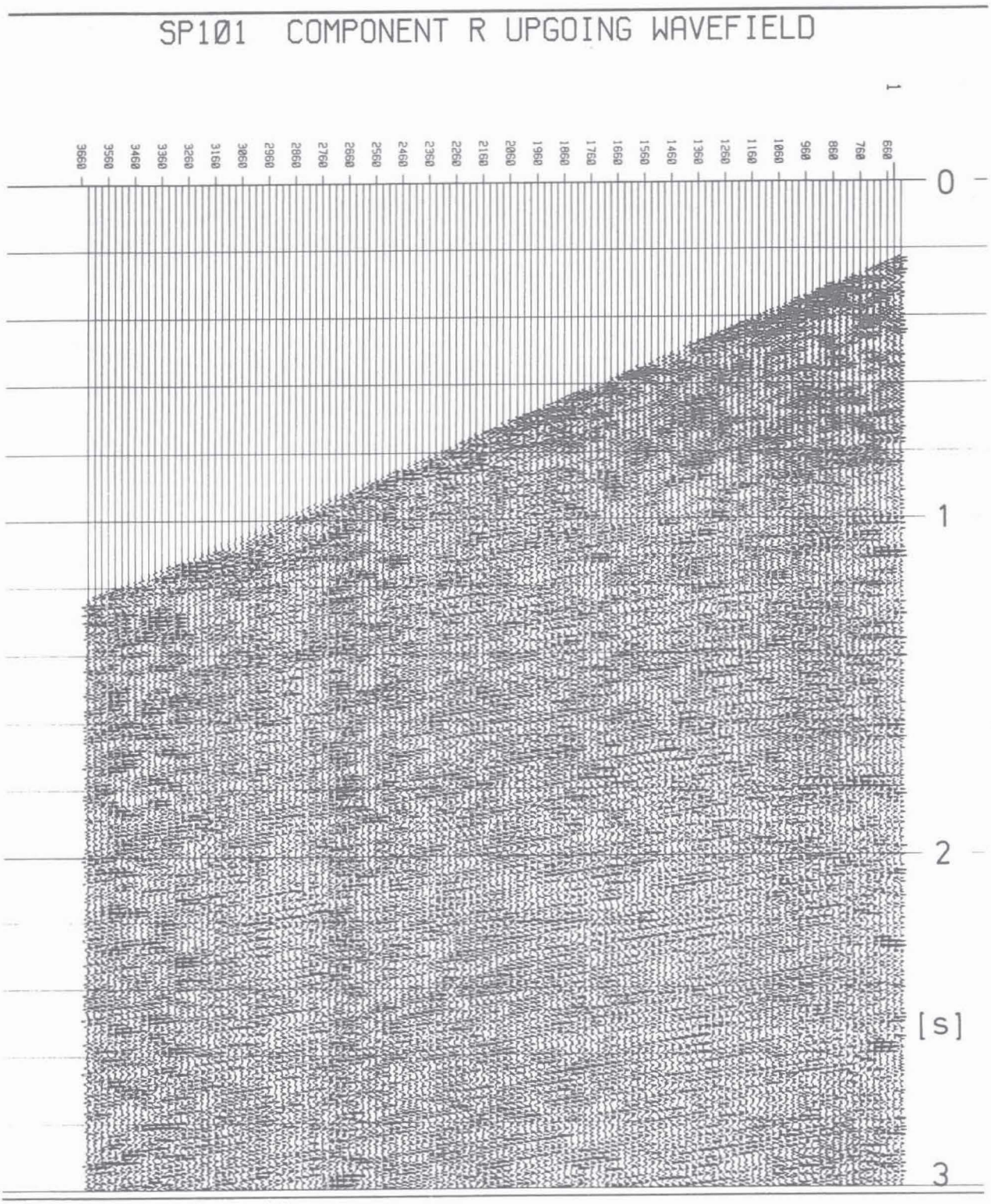
SP101 COMPONENT R UPGOING WAVEFIELD
1
3660
3560
3460
3360
3260
3160
3060
2960
2860
2760
2660
2560
2460
2360
2260
2160
2060
1960
1860
1760
1660
1560
1460
1360
1260
1160
1060
960
860
760
660
0
1
2
[s]
3

Fig 21

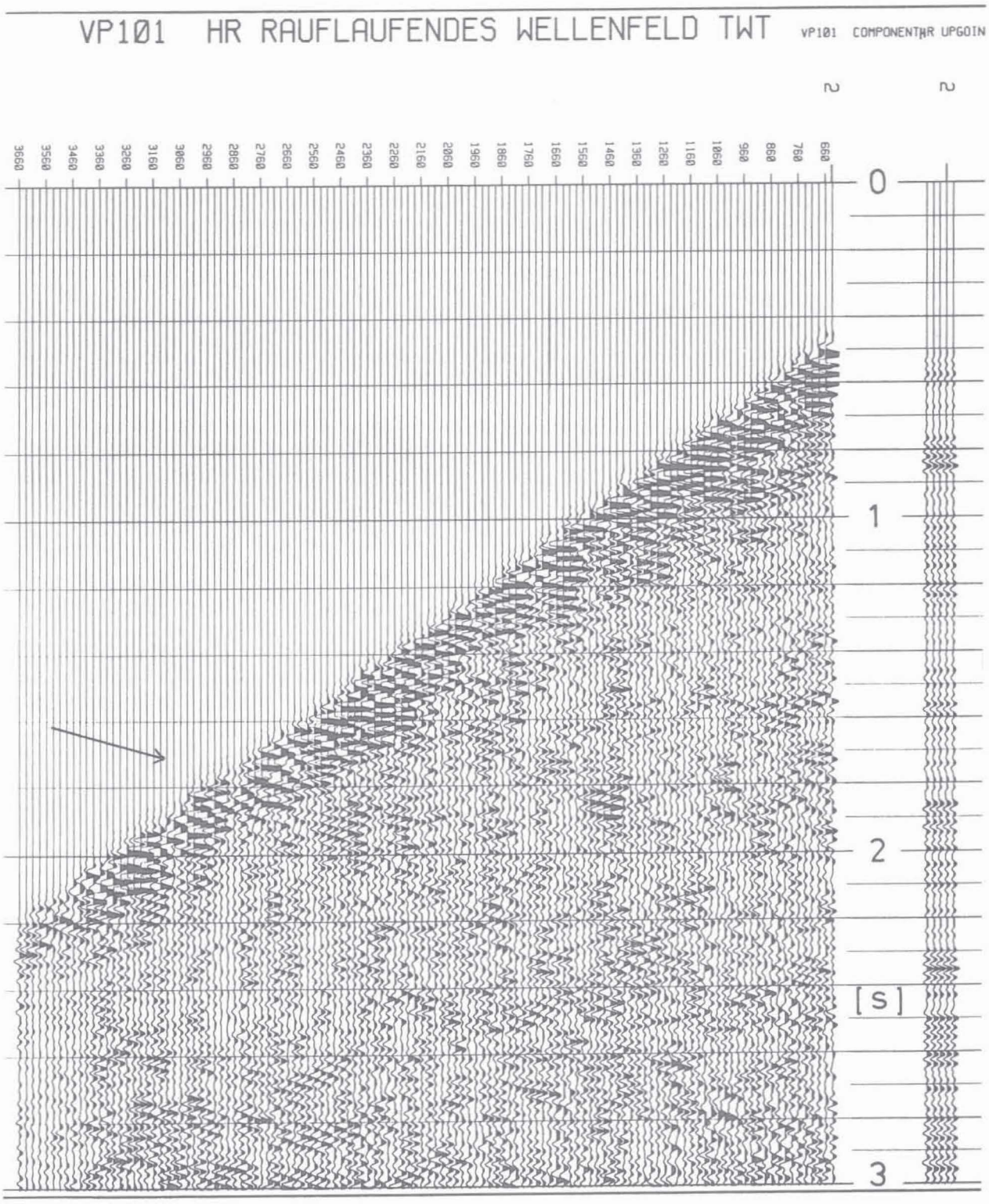
VP101 HR RAUFLAUFENDES WELLENFELD TWT
VP101 COMPONENTHR UPGOIN
3660
3560
3460
3360
3260
3160
3060
2960
2860
2760
2660
2560
2460
2360
2260
2160
2060
1960
1860
1760
1660
1560
1460
1360
1260
1160
1060
960
860
760
660
0
1
2
[s]
3

Fig 22

Figure 13a: Zero-offset vertical seismic profiles in comparison. Components are: 1=R, 2=HR, 3=HT (rotation with covariance matrix). Processing also includes deconvolution. Plotting is with AGC of 300 ms. Traces are time shifted in order to align S-wave first arrivals horizontally. From top to bottom: dynamite VSP 3600, dynamite SP 101, vertical vibrator VP 101 P, horizontal vibrator VP 101 S, Marthor MP 101 (after inverted stacking of left right shot). Note different energy of shearwaves and different frequencies. Timing lines in intervals of 200 ms.

Figure 13b: Blow-up of VSP 3600 (component HR). Compare figure 13a.

Figure 14: Enlarged section of VSP VP 101 P (vertical vibrator), N-component, AGC with 300 ms window length. Two splitted shearwaves are marked.

Figure 15: Particle motion diagrams (hodograms) for selected adjacent 3-component traces of figure 14. The hodograms correspond to the trace windows of 30 ms length marked on the left. Note that direction of particle motion changes from NW-SE to SW-NE within 60 ms.

Figure 16: Special experiment CIPHER. Raw data for a VSP between 2800 and 3400 m depth. Components 1=Z, 2=N, 3=E, rotated using compass readings.

Figure 17: Far-offset vertical seismic profiles, source location 401: 4 km offset, azimuth NE. Dynamite source SP 401 (top), bandpass 15-40 Hz, horizontal vibrator VP 401 (bottom), bandpass 18-35 Hz. Rotated with covariance matrix: components 1=R, 2=HR, 3=HT. No amplitude scaling, horizontal balancing applied.

Figure 18: Far-offset vertical seismic profiles, source location 402: 4 km offset, azimuth SE. Dynamite source SP 402 (top), bandpass 15-40 Hz, horizontal vibrator VP 402 (middle), bandpass 18-35 Hz. Source location 802: 8 km offset, azimuth SE, dynamite source SP 802 (bottom), bandpass 15-40 Hz. For rotation see figure 17, but the method was not successfull in case of SP 802 (bottom).

Figure 19: Upgoing wavefield of VSP 3600 after f-k filtering, radial component, in two-way-traveltime representation. Trace interval 12.5 m. For processing steps see text. Bandpass 40-90 Hz, AGC with 300 ms window for plotting. Summed traces (horizontal stack of all traces) on the right. Muting after f-k filtering along first arrival traveltime curve.

Figure 20: Sonic log of December 7th, 1988, provided by KTB logging group

Figure 21: Upgoing wavefield of SP 101 after f-k filtering. Trace interval 25 m. Bandpass 40-110 Hz. See figure 19 for more details.

Figure 22: Upgoing wavefield of VP 101 (shearwave vibrator) after f-k filtering, HR component, in TWT representation. Trace interval 25 m, Bandpass 18-35 Hz, AGC with 500 ms window for plotting. Summed traces (horizontal stack of all traces) on the right. The arrow marks an example of an upgoing tube wave (Stoneley wave, see text).

Figures 19, 21 and 22 correspond to the upgoing (reflected) wavefield after f-k filtering of the zero-offset profiles. We show examples from the 1988 experiment (Bram, 1988, Hohrath, 1990) in figure 19, the SP 101 for comparison (figure 21), representing the reflected P-waves, and VP 101 (figure 22), representing the upgoing S-waves. Processing is as described above. Figure 20 presents the sonic log for comparison.

In the VSPs of the crystalline environment fundamental differences are discernible compared to data from sedimentary strata. Instead of long continuous reflected branches, numerous shorter segments are visible. Only a few of them form long consistent branches, although often interrupted. We attribute this to a generally lower energy of reflections, hence a lower signal to noise ratio, which is caused by energy losses due to numerous small scale impedance contrasts. The wavefield therefore must be considered as an interference pattern or back-scattered energy from numerous single reflections.

Reflections from horizontal structures would show up parallel to the depth axis. Only one horizontal reflection is visible in figures 19 and 21, originating at 3200 m depth. The horizontal stack (see right side of figure 19) enhances this reflector, having a two-way-traveltime of 1.2 s. The sonic log (figure 20) shows a pronounced low-velocity peak at this depth, where a fracture zone is known from other borehole measurements and from coring, but it is characterized by a strong dip. Curiously, at the same depth in the VSP another reflection originates which is oblique to the depth axis, indicating a pronounced dip. It also reveals a curvature typical for reflections from dipping structures. It must be assumed that the fracture is responsible for the dipping reflector. The question arises about the nature of the horizontal reflector.

Consistent reflections are relatively poor above 2000 m, although shorter segments correlate with variations in the sonic log. Below 2000m depth, the intensity of the reflection pattern is generally increased. Inclined reflections showing the characteristic dip and a slight bending are dominating at all depth ranges. All possible dips are present, the steepest reflectors are visible in unfiltered versions, represented by downgoing waves behind the direct wave. In figure 21 most features of the VSP 3600 are confirmed, the dominance of dipping reflections (typically 30-40°) is drastically enhanced. The horizontal stack of all traces (see figure 19) selects the horizontal reflectors only, e.g. at 1.2 s, while all the inclined reflectors have been cancelled by this procedure. The 1.2 s reflector can be identified in the surface 2D section (see figure 2), while all the included reflections tend to be suppressed during standard CMP processing which emphasizes horizontal layering of structures. With this information from the VSPs, processing of 2D and 3D surface measurements could focus on dipping reflections using modified stacking velocities or dip move-out (DMO) stacking techniques.

In the S-wave VSP (figure 22) the upgoing wavefield is also characterized by dominating inclined events. Horizontal reflections are not recognized. Shearwave reflections from dipping structures (regardless of their strike) must be inclined toward the origin of the diagram. There are several events

with the opposite inclination. These can be interpreted unequivocally as borehole-guided waves (tube waves, Stoneley waves), because of their low phase velocity. All other upgoing wave types have to align horizontally (reflected S-wave from horizontal structure) or obliquely towards the origin at the surface. Borehole-guided waves bear the potential of information about the recent stress pattern and crack orientation. From systematic inspection of all down-going and upgoing wavefields of different types (after appropriate f-k filtering) we expect to characterize the medium and its impedance contrasts by mapping the P-reflections, P to S converted waves (down, up), S-reflections, S to P converted waves (down, up) and tube waves.

IV) MASE

The processing of the multiple azimuth shearwave experiment is basically the same described in case of the S-MSP (see above). Figure 23 displays the traces recorded with the vertical component of unit 2 in 3375 m depth. It is selected as an example out of 5 units located in 3300 to 3400 m depth, each one with 3 components. The traces represent the vibrator positions starting in the NW moving around the KTB-site on two different radii. The first group of traces (labelled 4 T, lefthand) are from transversal orientation of the S-wave vibrator on the 4-km-circle, the second group (4 R) from radial orientation, the same with the 8-km-circle. Static corrections have been applied which account for slight variations in the source-receiver distance. The reference distance is 5300 m for the 4-km-circle and 8700 m for the 8-km-circle. Variations in travelpath length (calculated with 3D coordinates of receiver and source) are reduced with an average S-wave velocity of 3070 m/s.

The shearwaves are the dominant phases on figure 23. The first S-wave clearly displays a traveltime anomaly consistently on both radii and both source orientations. As expected from azimuthal anisotropy, this anomaly has a sinoidal behaviour as a function of the azimuth. Conclusions in terms of anisotropy can be drawn after application of additional static corrections for near-surface effects. This is not yet available.

DISCUSSION

Systematic analysis of the polarization using variable source as well as three receiver components is expected to provide a quantitative image of seismic anisotropy, which may be caused by the recent stress pattern (Nur and Simmons, 1969), or by orientated fracture systems (Crampin, 1987b), by texture and foliation of the rock. The MASE provides observations variable in azimuth, but constant in offset. The S-MSP on the contrary allows for observations constant in two azimuths, but variable in offset. The VSPs complete the observation scheme with data variable in depth.

The initial results presented in this paper show a remarkable correlation with the orientation of the most compressive stress in the KTB deduced from televiewer observations (Mastin et al., 1990). The orientation of this stress field is almost N 160°. The azimuthal difference in P- and S-wave velocities observed in the SCMP survey (see table 3), the fastest waves

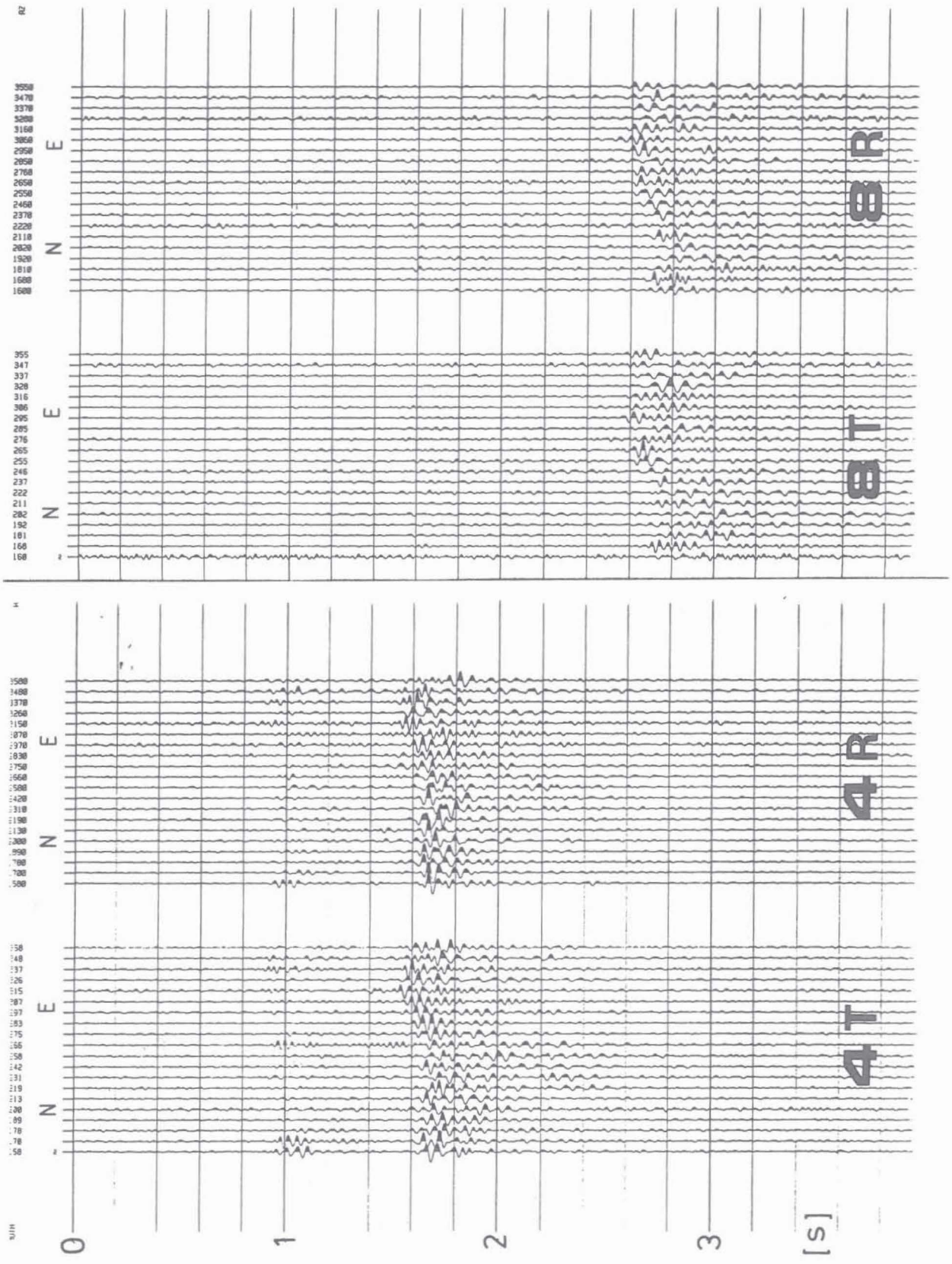

Fig 23

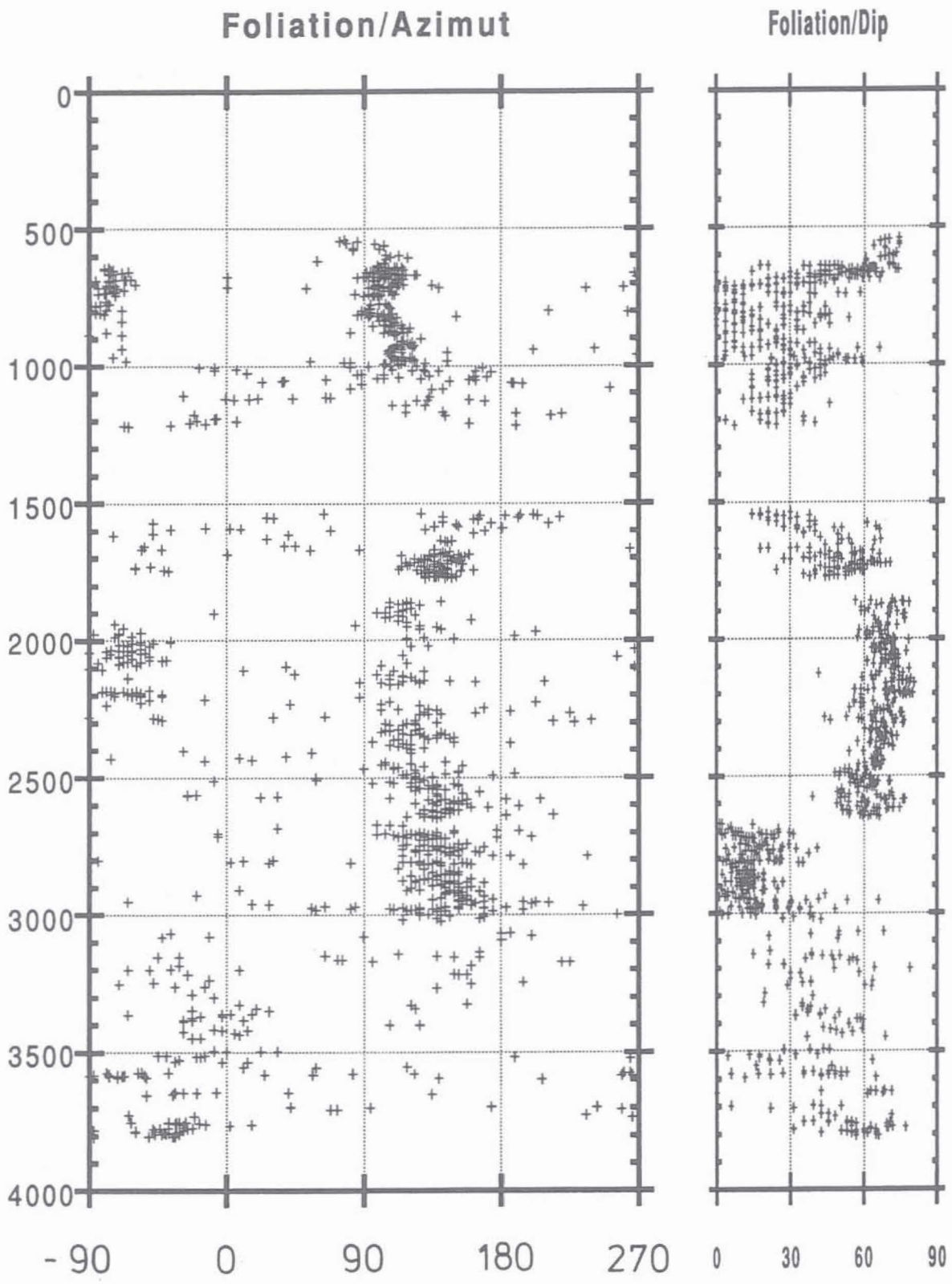
Foliation/Azimut
Foliation/Dip
0
500
1000
1500
2000
2500
3000
3500
4000
- 90
0
90
180
270
0
30
60
90

Fig 24

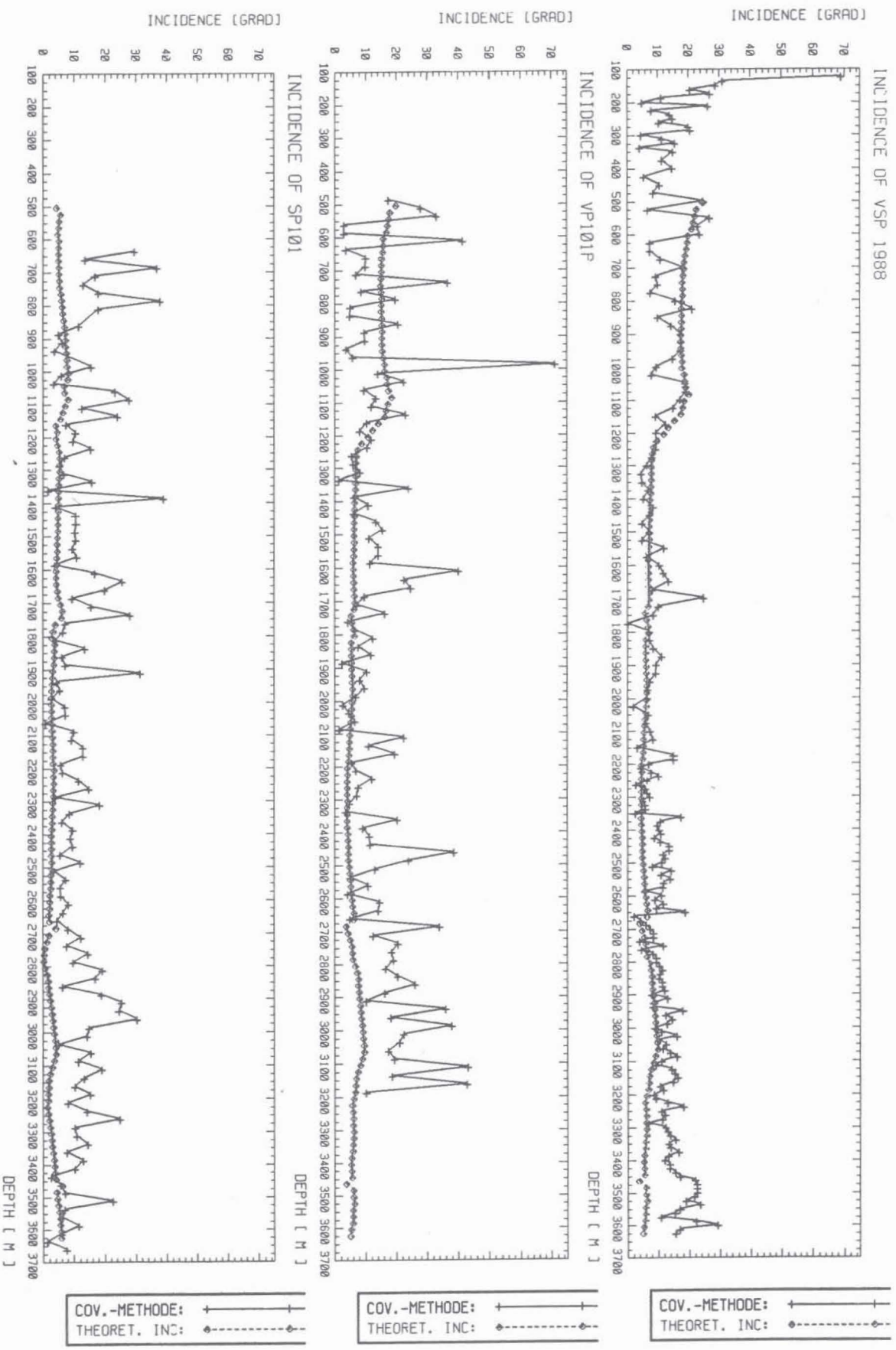
INCIDENCE [GRAD]
INCIDENCE OF VSP 1988
DEPTH [M]
COV.-METHODE:
THEORET. INC:
INCIDENCE [GRAD]
INCIDENCE OF VP101P
DEPTH [M]
COV.-METHODE:
THEORET. INC:
INCIDENCE [GRAD]
INCIDENCE OF SP101
DEPTH [M]
COV.-METHODE:
THEORET. INC:

Fig 25

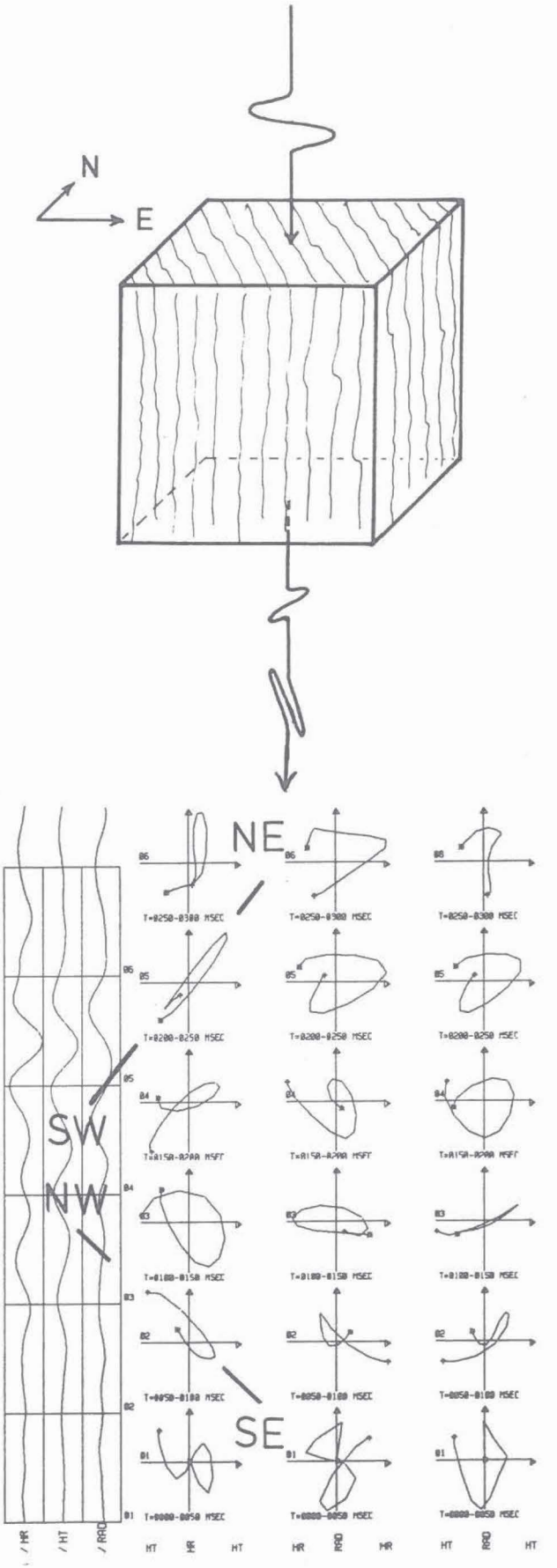
N
E
NE
SW
NW
SE
/ HR
/ HT
/ RAD
T=0250-0300 MSEC
T=0200-0250 MSEC
T=0150-0200 MSEC
T=0100-0150 MSEC
T=0050-0100 MSEC
T=0000-0050 MSEC
HT HR HT
HR RAD HR
HT RAD HT

Fig. 26

Figure 23: Multiple azimuth shearwave experiment. All traces in this example are from Z component of the second downhole unit of SEKAN 5 in 3375 m depth. From left to right: 4 km offset with transverse source orientation, 4 km offset with radial orientation, 8 km offset with transverse orientation, 8 km offset with radial orientation. In each panel the traces start on the left with the source location in the NW. Static corrections include correction for distance, but no near-surface effects at the source. True relative amplitudes.

Figure 24: Azimuth (left) und dip (right) of foliation in the KTB-borehole derived from televiewer measurements (courtesy borehole study group at Geophysical Institute Karlsruhe). Note steep foliation at 1500-2700 m depth striking N 140o. This is believed to cause shearwave splitting demonstrated in figures 14, 15 and 24.

Figure 25: Incidence of the direct P-wave determined by the covariance matrix (crosses) and by geometrical calculation in an isotropic medium (squares) versus depth. Panels from left to right: SP 101 (dynamite), VP 101 P (P-wave vibrator), VSP 1988 (dynamite). The anomaly at about 1100 m depth corresponds to a deviation of the borehole.

Figure 26: Schematic diagram showing the suggested effect of the rock foliation on shearwave splitting.
The lower part shows an example of the effect seen in particle motion diagrams of shearwave direct arrivals of VSP VP 101 S (S-wave vibrator).
Motion is first in NW-SE, then in SW-NE direction with a delay of nearly 150 ms.

being observed in NW direction, may be attributed to the stress field and to the possible preferred orientation of cracks, which are related to each other. This is very likely for the uppermost 1 or 2 km. The velocities deduced from the first arrivals of the SCMP survey also correspond to this depth range.

Below the upper depth range, particularly between 1500 and 3000 m, we suggest that shearwave splitting observed in figures 14 and 15 is mainly caused by rock foliation. Figure 24 displays strike direction and dip angle derived from borehole televiewer measurements. In the depth range between 1500 and 2700 m, the dip is almost vertical, the azimuth is about 150 to 160 degree. Figure 25 shows the incidence of the direct P-wave determined by the covariance matrix and the incidence calculated in an isotropic medium using the direct raypath. This theoretical incidence is corrected for the borehole deviation. The VSP 1988 data is to a high degree rectilinearily polarized whereas the VP 101 P and SP 101 data show lower rectilinearity, due to effects caused by the wheathering zone. Deviations between the two functions are expected to be related to interference of the direct P-wave with P to S converted and reflected wave modes as well as to deflections due to foliated rocks. Remarkable are the anomalies of the measured incidence angle below 2300 m in the VSP 1988, which might be caused by the increased number of reflections (see upgoing wavefield, figure 19) and variations in the foliation (figure 24).

Figure 26 the suggested relation between foliation and shearwave splitting is shown qualitatively. Cracks and microcracks with the same orientation can produce the same effects (Crampin, 1987b) and cannot be excluded here. Petrophysical investigations of Kern and Schmidt (1990) on core samples indicate that there is considerable velocity anisotropy dominated by crystallographic preferred orientation of major minerals (texture), in particular biotite and hornblende.

From systematic analysis of the polarization in the future, taking into account the variation of source orientations, offsets and azimuths at the surface and depth variations of the seismic wavefield, we expect more quantitative results on seismic anisotropy, its nature and its distinction from lateral heterogeneity. Further evaluation will be accomplished with reference to the other results of ISO89. The intention of this paper was to present the design of the field experiments and the presently existing data base.

REFERENCES

Benhama, A., Cliet, C., Dubesset, M. (1988): Study and applications of spatial directional filtering in three-component recordings. Geophysical Prospecting, 36: 591-613.

Bram, K. (1988): VSP-Messungen in der Bohrung KTB-Oberpfalz. In: Draxler and Haenel (Eds.), Grundlagenforschung und Bohrlochgeophysik (Bericht 5), KTB-Report 88-7.

Crampin, St. (1987a): Geological and industrial implications of extensive-dilatancy anisotropy. Nature, 328: 491-496.

Crampin, St. (1987b): Crack porosity and alignment from shear-wave VSPs. in: S.H. Danbom and S.N. Domenico (Editors), Shear-wave Exploration, Geophysical Developments, SEG Special Publ., 1, 227-251.

DEKORP Research Group (1988): Results of the DEKORP4/KTB Oberpfalz deep seismic reflection investigations. J. Geophys., 62: 69-101.

Danbom, S.H. and Domenico, S.N. (Editors) (1986): Shear-Wave Exploration. Geophysical Development Series, Vol.1, Society of Exploration Geophysicists, Tulsa, Okla., 274 p.

DiSiena, J.P., Gaiser, J.E. and Corrigan, D. (1984): Horizontal Components and shear wave analysis of three-component VSP data. in: Toksöz, M.N. Stewart, R.R. (Editors), Vertical Seismic Profiling, Part B: Advanced Concepts. Geophysical Press, London, p. 177-188.

Edelmann, H.A.K. (1985): Shear-wave energy sources. in: G. Dohr (Editor), Seismic Shear Waves, Part B, Applications. Geophysical Press, London, pp. 134-177.

Edelmann, H.A.K. and Lüschen, E. (1990): New shear wave technique first applied for deep crustal studies, in preparation.

Fertig, J. (1984): Shear waves by an explosive point-source: the earth surface as a generator of converted P-S waves. Geophysical Prospecting, 32: 1-17.

Franke, W. (1989): The geological framework of the KTB drill site, Oberpfalz. In: R. Emmermann, J. Wohlenberg (Eds), The German Continental Deep Drilling Program (KTB), Springer Verlag, Berlin, pp. 37-54.

Hardage, B.A. (1985): Vertical seismic profiling, Part A: principles. Handbook of Geophysical Exploration, Vol. 14A, Geophysical Press, London, 509 p.

Helbig, K. and Mesdag, C.S. (1982): The potential of shear-wave observations. Geophysical Prospecting, 30: 413-431.

Hohrath, A. (1990): VSP-Processing anhand einer Drei-Komponenten Registrierung im KTB. Diploma Thesis, University of Karlsruhe.

Kästner, U., Bram, K., Hubral, P., Kiefer, W., Köninger, Ch., Macdonald, C., Merz, J., Rühl, Th., Sandmeier, K.-J. (1989): Seismische Untersuchungen an der KTB-Lokation. KTB-Report 89-1, 169-210.

Kanasewich, E.R. (1981): Time sequence analysis in geophysics. The Univ. of Alberta Press, Winnipeg, pp. 480.

Kern, H. (1982): P- and S-wave velocities in crustal and and mantle rocks under the simultaneous action of high confining pressure and high temperature and the effect of the rock microstructure. In: W. Schreyer (Editor), High-Pressure Researches in Geoscience. Schweizerbartsche Verlagsbuchhandlung, Stuttgart, pp. 15-45.

Kern, H., Schmidt, R. (1990): Petrophysical investigations on KTB core samples at simulated in situ conditions. Poster presented at KTB-Kolloquium, Giessen, 28.2.-2.3.1990.

Mylius, J., Nolte, E., and Scharf, U. (1990): Use of the seismic receiver chain SEKAN 5 within the framework of integrated seismics in the Oberpfalz, this volume.

Lüschen, E., Wenzel, F., Sandmeier, K.-J., Menges, D., Rühl, Th., Stiller, M., Janoth, W., Keller, F., Söllner, W., Thomas, R., Krohe, A., Stenger, R., Fuchs, K., Wilhelm, H. and Eisbacher, G. (1987): Near-vertical and wide-angle seismic surveys in the Black Forest, SW Germany. J. Geophys, 62: 1-30.

Lüschen, E., Nolte, B. and Fuchs, K. (1990): Shear-wave evidence for an anisotropic lower crust beneath the Black Forest, southwest Germany. Tectonophysics, 173: 483-493.

Lüschen, E., Durrheim, R., Feddersen, J., Hopp, O. and Edelmann, H.A.K. (1990): A comparison of controlled shear-wave sources for crustal studies in southern Germany. In preparation for submission to Geophysical Prospecting.

Mastin, L., Heinemann, B., Krammer, A., Fuchs, K., Zoback, M.D. (1990): Stress orientation in KTB Pilot hole determined from wellbore breakouts. submitted to Scientific Drilling.

Nur, A., Simmons G. (1969): Stress-induced velocity anisotropy in rock: an experimental study. J. Geophys. Res., 74, 6667-6674.

Schruth, P., Bram, K., Hohrath, A., Hubral, P., Kästner, U., Lüschen, E., Rühl, T., Söllner, W. (1990): Auswertung und Interpretation der VSP-Messungen in der Bohrung KTB-Oberpfalz VB bis zu einer Tiefe von 3600 m. KTB-Report, in press.

Toksöz, M.N. and Stewart, R.R. (editors, 1984): Vertical Seismic Profiling, Part B: Advanced Concepts. Handbook of Geophysical Exploration, Vol 14B. Geophysical Press, London, 419 p.